Effects of changes in *TIA1* on stress granule formation

Master's thesis
Lydia Sagath
University of Helsinki
Faculty of Biological and Environmental Sciences
Genetics
August 2015

HELSINGIN YLIOPISTO
HELSINGFORS UNIVERSITET
UNIVERSITY OF HELSINKI

Tiedekunta – Fakultet – Faculty Bio- och miljövetenskapliga fakulteten	Laitos – Institution– Department Biovetenskapliga institutionen	
Tekijä – Författare – Author Lydia Johanna Sagath		
Työn nimi – Arbetets titel – Title Effects of changes in TIA1 on stress granule formation		
Oppiaine – Läroämne – Subject Humangenetik		
Työn laji – Arbetets art – Level Pro gradu	Aika – Datum – Month and year Augusti 2015	Sivumäärä – Sidoantal – Number of pages 63

Tiivistelmä – Referat – Abstract

Welanders distala myopati (WDM) orsakas av mutationen p.E384K i genen *TIA1*. Mutationen antas vara sjukdomsalstrande på grund av en ökad produktion av protein, som relaterats till formationen av stressgranuler (Hackman *et al.* 2013). Även omgivningsfaktorer har föreslagits verka i sjukdomens utveckling: en ökad mängd stressgranuler har observerats i celler som behandlats med köldshock jämfört med celler som förvarats i 37°C (Hofmann *et al.* 2012).

I patienter med WDM-liknande symptom som undersökts för förändringar i *TIA1* har en p.N357S-förändring noterats förrikad. Denna förändring har tidigare anmälts som en polymorfism. Förändringen i fråga ligger i samma prionliknande domän i exon 5 som WDM-orsakande förändringen p.E384K. Därmed kunde p.N357S-förändringen öka predispositionen till aggregering.

Pro gradu –arbetet är uppdelat i två delar:

- p.N357S-polymorfismens effekt på stressgranulsbildningen i arsenitbehandle celler
- Köldshockens effekt på stressgranulsbildningen

Resultaten påvisar, att förändringen p.N357S i TIA1 orsakar en förändring i det translaterade proteinets beteende. I likhet med p.E384K-förändringen orsakar även p.N357S en ökad mängd stressgranuler i arsenitbehandlade celler. Däremot tyder resultaten på att stressgranulerna återbildas snabbare i fluorescence recovery after photobleaching-studier (FRAP) I p.N357S-transfekterade celler än i celler som transfekterats med *TIA1* p.E384K och vildtyp.

Köldshocksexperimenten tyder på att det finns en viss skillnad mellan bildningen av stressgranuler i celler transfekterade med p.E384K och vildtyps-*TIA1*. Detta stöder tidigare publicerade resultat om p.E384K-förändringens påverkan på stressresponsen och stressgranulsbildningen, och även köldshock som stressinducerande behandling.

Använda metoder: PCR, transformation, DNA-ekstraktion, cellkultur, transfektion, induktion av stressgranulsformation med arsenitbehandling och köldshock. Cellerna kultiveras på brunnsplattor, fotograferas och datat analyseras med en automatiserad High Content biildanalysmetod (CellInsight-platform). p.N357S-celler analyserades även med FRAP.

Avainsanat – Nyckelord – Keywords
TIA1, stressgranul, Welanders distala myopati

Ohjaaja tai ohjaajat – Handledare – Supervisor or supervisors
Per Harald Jonson, Peter Hackman, Jaakko Sarparanta

Säilytyspaikka – Förvaringställe – Where deposited

Muita tietoja – Övriga uppgifter – Additional information

HELSINGIN YLIOPISTO
HELSINGFORS UNIVERSITET
UNIVERSITY OF HELSINKI

Tiedekunta – Fakultet – Faculty Faculty of Biological and Environmental Sciences	Laitos – Institution– Department Department of Biosciences	
Tekijä – Författare – Author Lydia Johanna Sagath		
Työn nimi – Arbetets titel – Title Effects of changes in TIA1 on stress granule formation		
Oppiaine – Läroämne – Subject Human genetics		
Työn laji – Arbetets art – Level Pro gradu	Aika – Datum – Month and year August 2015	Sivumäärä – Sidoantal – Number of pages 63

Tiivistelmä – Referat – Abstract

Welander Distal Myopathy (WDM) is caused by the p.E384K mutation in the *TIA1* gene. The mutation supposedly causes the disease by a gain-of-function mechanism related to the formation of stress granules (Hackman *et al.* 2013). Also environmental factors have been proposed to affect the development of the disease: an increased number of stress granules has been observed in cells treated with cold shock compared to cells kept in 37 °C (Hofmann *et al.* 2012).

When patients with WDM-like symptoms have been screened for changes in TIA1, an p.N357S-change has been found enriched in these patients. The p.N357S-change has earlier been reported as a polymorphism. The change in question is located in the same prion-like domain in exon 5, in which the p.E384K-mutation also lies. Therefore, the p.N357S-change could affect the predisposition to aggregation.

The pro gradu project is divided into two parts:

- The effect of the p.N357S polymorphism on stress granule formation in arsenite and possibly other stress treated cells
- The effect of cold shock on stress granule formation on wild type and p.E384K TIA1

The results indicate, that the p.N357S change in TIA1 causes a change in the translated protein's behavior. Similarly to the p.E384K change, the p.N357S change also induces an increased amount of stress granules in arsenite treated cells. However, the results also show that the stress granules recover faster in fluorescence recovery after photobleaching (FRAP) studies p.N357S transfected cells as compared to *TIA1* p.E384K and wild type transfected cells.

The cold shock experiment indicates that there is a difference in the stress granule formation between cells transfected with p.E384K and wild type TIA1. This supports previously published results of the effect of the p.E384K change on the stress response and stress granule formation, and also the use of cold shock as a stress inducing treatment.

Used methods: PCR, transformation, DNA-extraction, cell culture, transfection, induction of stress granule formation by arsenite treatment and cold shock. The cells are cultivated on well plates, imaged and the data is analyzed with an automatized high content image analysis method (the CellInsight-platform). p.N357S cells were also analyzed with FRAP.

Avainsanat – Nyckelord – Keywords TIA1, stress granule, Welander Distal Myopathy
Ohjaaja tai ohjaajat – Handledare – Supervisor or supervisors Per Harald Jonson, Peter Hackman, Jaakko Sarparanta
Säilytyspaikka – Förvaringställe – Where deposited
Muita tietoja – Övriga uppgifter – Additional information

INDEX

ABBREVIATIONS

40S	small ribosomal subunit
4ET	eukaryotic translation initiation factor 4E protein
60S	large ribosomal subunit
AD	autosomal dominant
Ago2	argonaute-2 protein
ANO5	anoctamin-5 gene
AR	autosomal recessive
bp	base pair
BRF-1	butyrate response factor 1 protein
CK	creatine kinase
CPEB	cytoplasmic polyadenylation element binding protein
CRYAB	alpha-crystallin B chain gene
CTL	cytolytic lymphocyte
DDX6	probable ATP-dependent RNA helicase DDX6 protein
DES	desmin gene
DIS1	microtubule-associated protein family
dNTP	deoxyribonucleosideditriphosphate
DYSF	dysferlin gene
eIF	eukaryotic initiation factor
EMG	electromyogram
ER	endoplasmic reticulum
FAST	FAS-activated serine/threonine kinase
FBP	folate-binding protein
FLNC	filamin C gene
FMRP	fragile X mental retardation protein
FRAP	fluorescence recovery after photobleaching
FXR1	fragile X mental retardation, autosomal homolog 1 protein
G3BP	GTPase activation protein (SH3 domain) binding protein
GCN2	general control nonderepressible 2 protein
GDP	guanosine di-phosphate
GNE	glucosamine(UDP-N-acetyl)-2-epimerase/N-acetylmannosamine kinase gene
GTP	guanosine tri-phosphate

Hedls	beta propeller protein Hedls
HRI	heme-regulated eIF2α kinase protein
kb/kbp	kilo base pairs (one thousand base pairs)
kDa	kiloDalton, one thousand Dalton (1 Da ≈ 1.660 x 10^{-24} g)
KLHL	Kelch-like gene family
KSRP	KH-type splicing regulatory protein
LBD3	LOB domain-containing protein 3
Lin28	lin-28 homolog protein
LINE1	long interspersed element 1 protein
MATR3	matrin3 protein
MD	muscular dystrophy
MLN51	metastatic lymph node 51 RNA-binding protein
MRI	magnetic resonance imaging
mRNA	messenger RNA
mTOR	mammalian target of rapamycin
MYH7	Myosin, Heavy Chain 7, Cardiac Muscle, Beta gene
NEB	nebulin gene
OMIM	Online Mendelian Inheritance of Man
ORF	open reading frame
p	short arm of the chromosome
PABP	poly(A)-binding protein
PBS	phosphate-buffered saline
PCR	polymerase chain reaction
PDZ	protein, acronym of PSD95, Dig1 and zo-1
PERK	pancreatic eIF2α-kinase protein
PFA	paraformaldehyde
PKR	protein kinase R protein
PMR	histone-like protein H1 family protein
q	long arm of the chromosome
SG	stress granule
smg	smaug protein
SMN	survival motor neuron protein
SNP	single nucleotide polymorphism
SRC3	steroid receptor coactivator 3 protein

Rap55	RNA-associated protein 55
RISC	RNA-induced silencing complex
Rpb4	RNA polymerase II subunit B4
RRM	RNA recognition motif
RV	rimmed vacuole
TFI	tubulofilamentous inclusions
TMD	tibial muscular dystrophy
TIA1	TIA1 cytotoxic granule-associated RNA-binding protein gene
TIAL	TIA1 cytotoxic granule-associated RNA-binding protein-like gene
TIAR	TIA1 cytotoxic granule-associated RNA-binding protein-like protein
TRAF2	TNF receptor-associated factor 2 gene
tRNA	transfer RNA
$tRNAi^{Met}$	initiator methionine transfer RNA
TTN	titin gene
TTP	tristetrapolin protein
UTR	untranslated region
VCP	valosin containing protein gene
WDM	Welander Distal Myopathy
YB-1	Y-box binding protein
ZASP	Z-band alternatively spliced PDZ-motif protein
ZBP-1	Z-DNA-binding protein 1

1. INTRODUCTION

Welander Distal Myopathy (WDM) is a dominantly inherited late-onset distal muscular dystrophy, which can also occur sporadically (Welander 1951). The disease has been encountered only in Finland, Sweden and one family in Great Britain (Hackman *et al.* 2013). The causative mutation was pinpointed in 2013 to a single nucleotide polymorphism (SNP) in the gene *TIA1 cytotoxic granule-associated RNA-binding protein* (*TIA1*), causing changes in the behavior of the gene product (TIA1) in stress conditions (Hackman *et al.* 2013).

TIA1 shuttles between the nucleus and cytoplasmic protein-RNA aggregates called stress granules (SG). SGs form as a result of the cells stress response (Anderson and Kedersha, 2008, and are measurable in both size and number when a fluorescent tag, such as GFP, is added to the TIA1 protein. Changing cell culture conditions can induce the stress response, and thus the formation of SGs.

The thesis is divided into two parts:

- Subproject I is aimed at researching the behavior of a SNP (p.N357S) enriched in patients with symptoms similar to those of patients with WDM by transfecting HeLa cells (derived from human cervical cancer) with TIA1 wild type and p.N357S. Subsequently, a stress response is induced by treating the cells with sodium arsenite, and the change in SG formation is studied.

- Subproject II, is aimed at researching the effect of cold shock in HeLa cells transfected with TIA1 wild type and TIA1 harboring the WDM-causing mutation p.E384K. The cold shock has been proven to induce a stress response (Hoffmann *et al.* 2012) and the aim is to study whether the WDM-causing mutation also changes the stress response in cold shock treated cells.

This thesis work was conducted at the Folkhälsan Institute of Genetics in the research group of neuromuscular diseases led by Professor Bjarne Udd. The supervisors of the work were Docent Peter Hackman, PhD Per Harald Jonson and FD Jaakko Sarparanta from the Udd group at the Folkhälsan Institute of Genetics. Imaging studies were done at the Biomedicum Imaging Unit and the Institute of Biotechnology Light Microscopy Unit at the University of Helsinki. Sequencing was performed by the Institute for Molecular Medicine Finland (FIMM). The work was funded by Samfundet Folkhälsan i svenska Finland rf and Jane and Aatos Erkko foundation.

2. SKELETAL MUSCLE

There are three types of muscle tissue in the human body: skeletal, cardiac and smooth muscles. Skeletal muscles are used for voluntary controlled movement under the somatic nervous system, whilst cardiac and smooth muscle tissues are used for involuntary movements, such as the contraction of the heart and peristaltic movements in the gastrointestinal tract (Alberts *et al.* 1994). Of these types of muscle tissue, the skeletal and cardiac muscle tissue are considered striated due to their organized composition (Craig and Padron, 2004).

The average human body consists of about 40% in mass of striated, skeletal muscle (Marieb and Hoehn 2010). As its name indicates, skeletal muscle is connected to the skeleton (usually by tendons) as to allow contractions in the tissue to create movement in parts of the body in reference to the body itself (MacIntosh *et al.* 2006). The number of muscle cells in adult mammals is fixed. Muscle mass can therefore be built only by enlarging existing muscle cells, instead of increasing their number (Campbell *et al.* 2008).

Skeletal muscle tissue can be divided into two major groups, the slow, oxidative type I and the fast, glycolytic type II muscle fibers. The human skeletal muscles are composed of a mixture of these two types (Silverthorn 2010). The type I is mainly found in large muscles meant for aerobic and long term activity and therefore contain many mitochondria and much myoglobin. The type II fibers are further divided into three different groups according to the neuron that innervates the motor unit:

i) Type IIA: produces energy either aerobically or anaerobically

ii) Type IIB: produces energy anaerobically, can produce powerful yet short contractions

iii) Type IIX: produces energy by lactic acid fermentation, produces fast contractions but not for long periods of time (Stone and Stone 2006).

Striated, skeletal muscle consists of organised bundles of muscle fibers (**Fig. 1)**. These fibers are large single cells (Ø = 10–100 μm) with multiple nuclei that form by fusion of smaller muscle cells. In healthy muscle cells, the nuclei are located on the edges of the cell, beneath the plasma membrane, to make room in the cytoplasm for the contractile element of the muscle, called the myofibrils (Ø = 1–2 μm). The cylindrical myofibrils span typically from one end of the cell to the other. Several contractile units of about 2.2 μm in length, called sarcomeres, build up each myofibril (Silverthorn 2010).

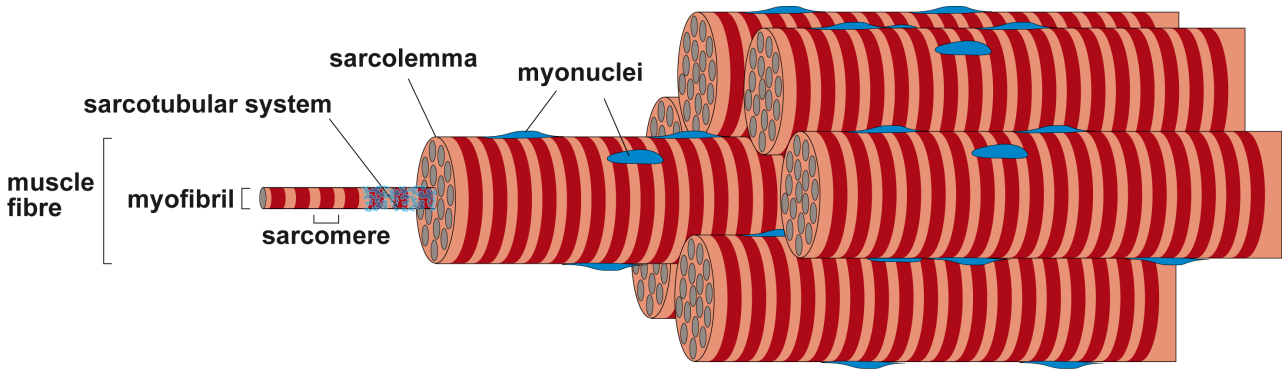

Figure 1. The structure of a striated muscle fiber. (Reprinted with permission from Jaakko Sarparanta)

Sarcomeres contain actin and myosin filaments that alternately overlap each other and give the muscle its striated look of alternating light and dark bands, visible in a light microscope (Craig and Offer 2004). The bands are separated by Z-discs, located in the middle of the light bands, and M-lines, located in the middle of the dark bands. The actin and myosin filaments are connected to the Z-discs and M-lines respectively (Alberts *et al.* 2002). The structure of the sarcomere is shown in **Fig. 2**.

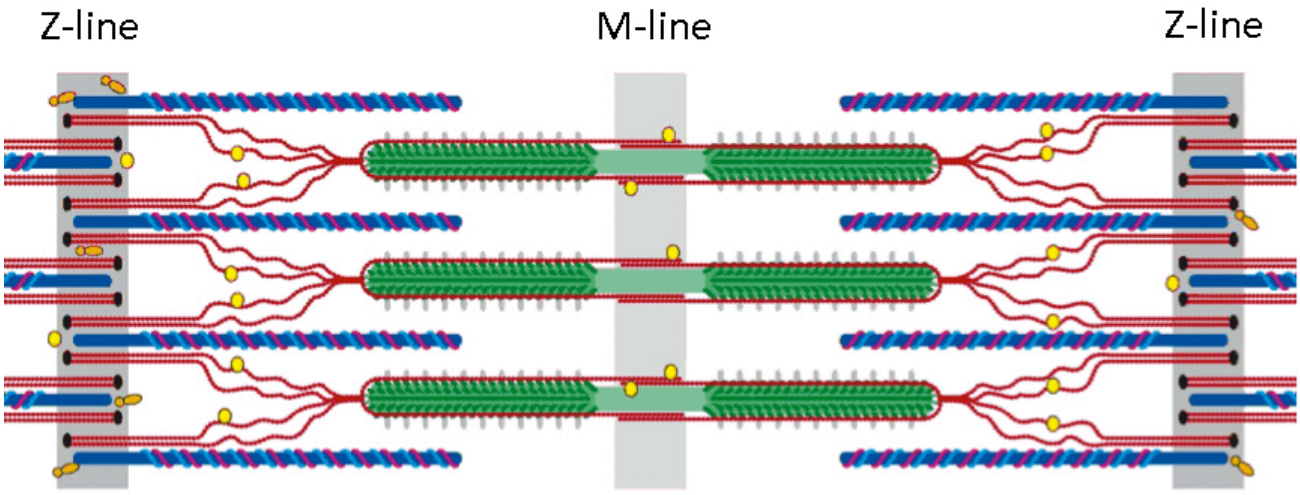

Figure 2. The structure of the sarcomere. Myosin shown in green, actin filaments in blue. (Reprinted with permission from Jaakko Sarparanta)

3. MUSCULAR DYSTROPHIES

Muscular dystrophies are a widely varying group of inherited myogenic disorders. The main trait of these disorders is a progressively weakening musculoskeletal system and the reduced mobility that follows. Generally the weakness is presented in a limb-girdle pattern, but some myopathies cause distal weakness, which may easily be mistaken for a neurogenic feature (Illa 2000).

Several different types of muscular dystrophies have been identified as separate disorder groups based on clinical investigations, such as the results of muscle biopsies, creatine phosphokinase (CK) levels in blood, electromyography, electrocardiography and lately by DNA analysis. Among the identified disorders and disorder groups are Duchenne, Becker, limb-girdle, congenital, fascioscapulohumeral, myotonic, oculopharyngeal, distal and Emery-Dreifuss muscular dystrophy. These disorders can be further grouped by the muscle groups affected into six major forms (**Fig. 3**). Nonetheless, the ages of onset, speed of progression and severity of the diseases vary even inside each group (Illa 2000).

As of yet, there are few pharmacological treatments for the disorders, and no way of affecting the long-term course of the diseases to an eminent degree has been found. Recent advances in gene manipulation and stem-cell therapy may provide treatment to patients in the future, but cautious optimism is advised (Emery 2002).

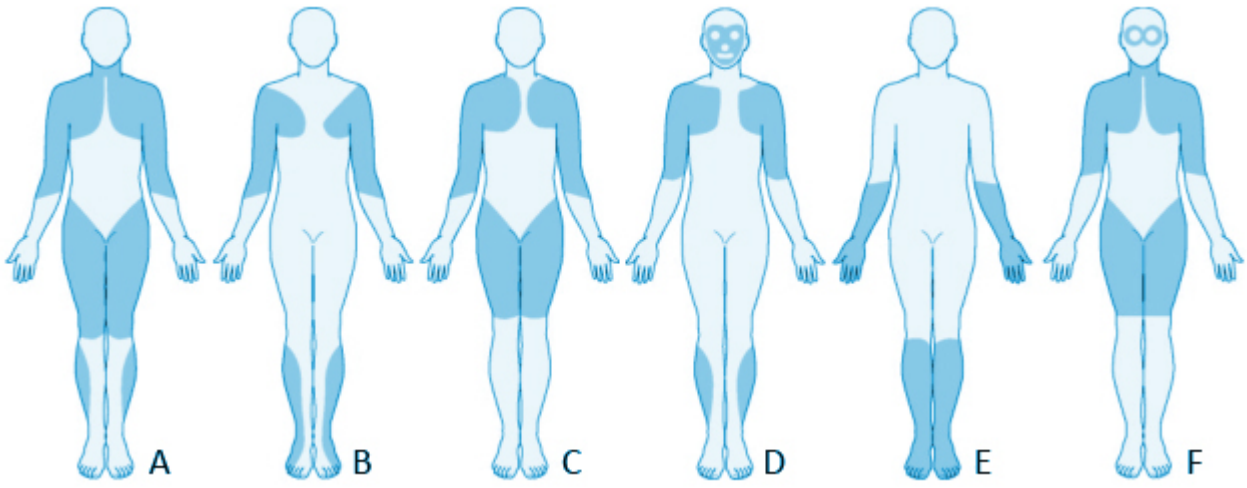

Figure 3. Depiction of affected muscles in different muscular dystrophies. A. Duchenne-type and Becker-type; B. Emery-Dreifuss; C. limb-girdle; D. Fascioscapulohumeral; E. Distal; F. Oculopharyngeal. Affected areas are shaded. Adapted from Emery, 2002.

4. DISTAL MYOPATHIES

Distal myopathies are a heterogeneous group of muscular dystrophies, which are inherited or occurring as sporadic muscular diseases. The common feature is muscular weakness and atrophy that progresses from the distal muscles of the extremities towards the proximal muscles closer to the body (Griggs *et al.* 1994).

The first distal myopathy was thoroughly described in 1951 by Lisa Welander, and she was also the first to establish the existence of distal myopathies, as opposed to the limb-girdle pattern of proximal dystrophies (Welander 1951). Her publication is considered the landmark publication for distal myopathies, although the very first case description of a distal muscular dystrophy is often attributed to Gowers in 1902 (Gowers 1902, Mastaglia 1999). The first distal muscular dystrophy gene, *dysferlin* (*DYSF*), was identified in 1998 (Illa 2000).

4.1 CLINICAL ASPECTS

Distal myopathies are diagnosed using several different methods to assess the condition of the patient's affected skeletal muscle tissue and motor neurons. This is done by a series of tests such as, electromyography (EMG), blood tests, magnetic resonance imaging (MRI) and biopsy examination. Reviewing patient family disease history also contributes to the diagnostic process (Borg *et al.* 1991).

Since distal myopathies are normally caused by an inherited genetic feature, patient family history is taken into account in detail. Some distal myopathies are however caused by a sporadic change, thus the possibility of a distal myopathy cannot be excluded solely based on the lack of disease occurrence in the patients family.

EMG is a diagnostic method, which is used to measure the electrical activity in the skeletal muscles. The aim of the technique is to assess whether the muscle weakness is caused by changes in muscle tissue (myopathy) or the nerves controlling it (neuropathy) (Logigian *et al.* 2010).

Blood tests include creatine kinase (CK) level analysis as default in patients with a suspected myopathic condition. Elevated CK levels are often, but not always, seen in patients with muscle disorders. CK is an enzyme functioning as an energy reservoir in tissues that are highly dependent on adenosine triphosphate (ATP) as their source of energy. Skeletal muscle is a prime example, but

several different tissues fall into this category – among them, the brain and the photoreceptor cells of the retina. High levels of CK in the blood indicates damage to such tissues, but is alone not a basis for diagnosis of a myopathy, since it could be caused by damage to other ATP-dependent tissues. In addition, not all myopathies lead to an elevated CK level in the patient (Hilton-Jones *et al.* 2010).

MRI is used to assess anatomical and physiological aspects of a patient using strong magnetic fields. Different distal myopathies cause distinct muscle weakness patterns, which can be identified with MRI of the muscles (Logigian *et al.* 2010).

In terms of histological changes, distal myopathies show a large variation of changes in the affected muscles. Muscle fiber necrosis (dead muscle fibers), split muscle fibers, internal nuclei, inclusion bodies and rimmed vacuoles (multilaminated vacuole-like constructs) are some of the most characteristic features indicating muscle damage (Illa 2000).

Patients with distal myopathies show myopathic changes in electromyography (EMG) studies and often have an elevated creatine kinase (CK) level in blood tests. Histological changes in muscle biopsies vary to a large degree, and are mainly nonspecific. No change has been observed in nerve conduction studies in distal myopathy patients – neural involvement is a feature of neuropathies or some other neuromuscular diseases (Illa 2000).

4.2 CLASSIFICATION

Only a few distal myopathies had been described and identified before the new era of molecular genetics. Now, at least 20 different distal myopathies have been separated into distinct disorders. In some of these cases, the underlying genetic changes are still unknown (Udd 2012).

Being a widely varying group of disorders, there are several ways in which to classify distal myopathies. In **Fig. 4 and Table 1** a traditional classification for the six major distal myopathy types (Tibial muscular dystrophy, Myofibrillar myopathy 4, Welander distal myopathy, Laing myopathy, Nonaka myopathy and Miyoshi muscular dystrophy) is shown. This sort of classification takes into account the mode of inheritance, the muscle groups affected and the age of onset, which are traditional clinical forms of investigation.

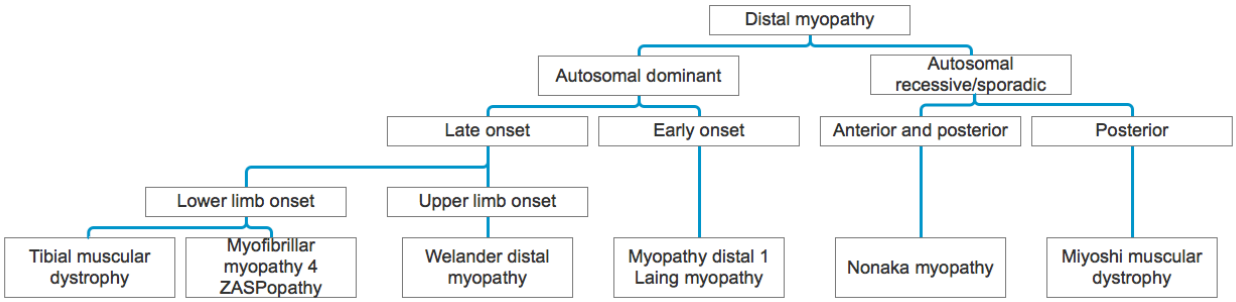

Figure 4. Traditional classification of the six major distal myopathy types. Adapted from Mastaglia, 1999 and Udd 2012.

Table 1. The major six forms of distal myopathies classified according to distinguishing features by their established scientific names. Adapted from Mastaglia 1999.

	WDM	TMD	MFM4	MPD1	NM	MMD1
OMIM #	604454	600334	609452	160500	605820	254130
Inheritance	AD	AD	AD	AD	AR/sporadic	AR/sporadic
Gene	*TIA1*	*TTN*	*LDB3*	*MYH7*	*GNE*	*DYSF*
Age of onset	>40	>35	25-50	4-25	20-30	15-30
Site of onset	Hands	Legs	Legs	Legs	Legs	Legs
Leg compartment	Anterior	Anterior	Anterior	Anterior	Both	Posterior
Proximal weakness	-	+ (late)	+ (late)	+	+ (late)	+ (late)
Neck weakness	-	-	-	+	+	+ (late)
CK	N or mild ↑	N or mild ↑	2-5X	<3X	<5X	10-100X
Myopathic	+	+	+	+	+	+
Spontaneous activity	+	+	+	+	+	+
RV's and TFI	+	+	?	-	+	-
Fiber necrosis	-	+	+	+	-	+

AD = autosomal dominant, AR = autosomal recessive, MFM4 = Myofibrillar Myopathy 4/ZASPopathy, MMD1 = Miyoshi muscular dystrophy, MPD1 = Myopathy Distal 1 (Laing myopathy), N = normal, NM = Nonaka Myopathy, OMIM = Online Mendelian Inheritance in Man, RVs = Rimmed vacuoles, TFIs = tubulofilamentous inclusions, TMD = Tibial Muscular Dystrophy WDM = Welander Distal Myopathy.

The methods of molecular biology have advanced rapidly during the last years. With the increased understanding of the genetic backgrounds and molecular pathomechanisms of distal myopathies, it has been suggested that the disorders should be categorized not necessarily by phenotype, but rather by the disease causing gene mutations. The traditional classification is restricted to only mode of inheritance, age of onset and the first muscle groups affected. Clinical symptoms, such as those above, give clues as to which category the patient may fall, but as both genetic factors and phenotypic traits can vary widely throughout patients, these principles start to be out-dated (Malicdan and Nonaka 2008).

Since there is an overlap in phenotypes and a large increase of identified disorders, a classification based on the genetic background of the disease could be of use (Udd 2012). A guideline for pinpointing the underlying genetic variations that cause certain clinical features is given in **Fig. 5**.

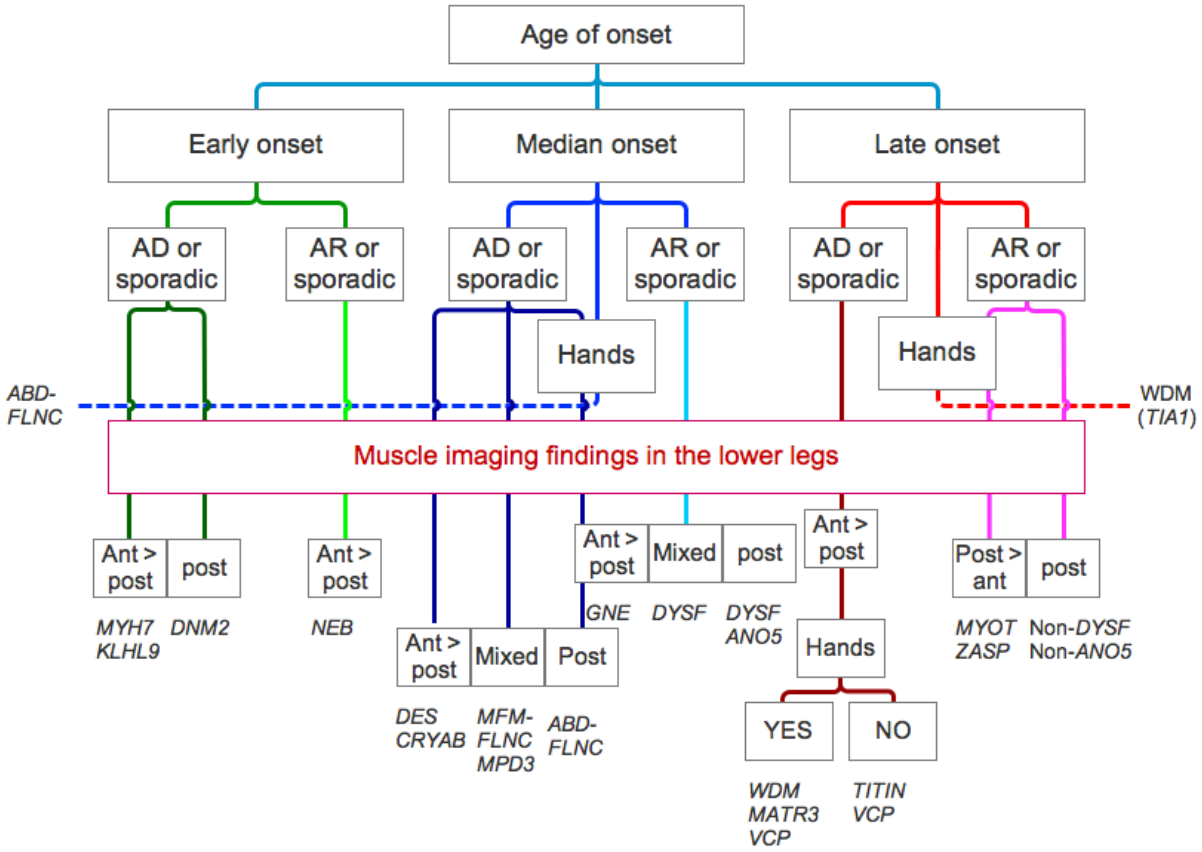

Figure 5. A general guideline to determine possible loci for genetic variation classed by clinical features. Genes are displayed in italics. AD = autosomal dominant, Ant = anterior onset, AR = autosomal recessive, Post = posterior onset, Adapted from Udd, 2012.

As inherited disorders, all distal myopathies are caused by genetic mutations in the DNA. Often, these proteins are expressed in the sarcomeres, the sarcoplasm, the cytoskeleton and the cytoplasm (Malicdan and Nonaka, 2008).

A more recent summary of distal myopathies and the genes and proteins related to them are shown in **Table 2**.

Table 2. Genetically determined distal myopathies. Adapted from Udd, 2012.

	Gene/Protein	OMIM	Reference
1. Late adult onset autosomal dominant forms			
a. Welander distal myopathy	*TIA1*/TIA1	#604454	Welander 1951, Hackman 2013
b. Tibial muscular dystrophy (TMD, UDD myopathy)	*TTN*/Titin	#600334	Udd *et al.* 1993
c. Distal myotilinopathy	*MYOT*/Myotilin	#609200	Pénisson-Besnier *et al.* 2006
d. ZASPopathy (Markesbery-Griggs)	*LDB3*/ZASP	#605906	Griggs *et al.* 2007
e. Matrin3 distal myopathy (VCPDM, MPD2)	*MATR3*/Matrin3	#606070	Senderek *et al.* 2009
f. VCP-mutated distal myopathy	*VCP*/VCP	N/A	Palmio *et al.* 2011
g. Alpha-B crystalline mutated distal myopathy	*CRYAB*/ αB-crystallin	N/A	Reichlich *et al.* 2010
2. Adult onset autosomal dominant forms			
a. Desminopathy	*DES*/Desmin	#601419	Sjöberg *et al.* 1999
b. Distal ABD-filaminopathy	*FLNC*/Filamin-C	#614065	Duff *et al.* 2011
c. Finnish-MPD3	Unknown	%610099	Mahjneh *et al.* 2003
d. Italian 19p13-linked distal myopathy	Unknown	%601846	Servidei *et al.* 1999
e. US-Polish family	Unknown	N/A	Felice *et al.* 1999
f. Oculopharyngeal distal myopathy OPDM	Unknown	%164310	Durmus *et al.* 2011
3. Early onset autosomal dominant forms			
a. Laing distal myopathy (MPD1)	*MYH7*/Beta-MyHHC	#160500	Laing *et al.* 1995
b. KLHL9 mutated distal myopathy	*KLHL9*/KLHL9	N/A	Cirak *et al.* 2010
4. Early onset autosomal recessive forms			
a. Distal nebulin myopathy	*NEB*/Nebulin	#256030	Wallgren-Petterson *et al.* 2007
5. Early adult onset autosomal recessive forms			
a. Miyoshi myopathy (MM)	*DYSF*/Dysferlin	#254130	Miyoshi *et al.* 1986
b. Distal Anoctaminopathy	*ANO5*/Anoctamin-5	#613319	Bolduc *et al.* 2010
c. Distal myopathy with rimmed vacuoles (Nonaka)	*GNE*/GNE	#605820	Noanka *et al.* 1981
d. Oculopharyngeal distal myopathy, OPDM	Unknown	%134310	Durmus *et al.* 2011
6. Adult onset autosomal recessive form			
a. Calf myopathy non-DYSF/ANO5	Unknown	%613318	Linssen *et al.* 1998

5. WELANDER DISTAL MYOPATHY

Welander Distal Myopathy (WDM, MIM #604454) is an autosomal, dominantly inherited late onset muscular dystrophy prevalent in Sweden and certain parts of Finland. Patients experience the first symptoms at around 50 years of age (40–60 y). The disease causes progressive muscular weakness in the distal muscles (Welander, 1951).

In 1951 Lisa Welander published a report, which knocked down earlier skepticism around the existence of a myopathy that would predominantly affect distal muscles in the body, as opposed to myopathies that cause weakness in proximal muscles. She studied 249 affected individuals from 72 separate pedigrees, mainly from central parts of Sweden (Welander 1951). A Swedish group mapped WDM to chromosome 2p13 in 1999 (Åhlberg *et al.* 1999). In 2013 a mutation in the RNA-binding protein TIA1 was identified to be the WDM causing factor (Hackman *et al.* 2013).

5.1. CLINICAL IMAGE

WDM is a late onset disease, with the first symptoms of muscular weakness setting in at between 40 and 60 years of age, affecting men and women equally. Patients experience weakness primarily in the small muscles and extensors of hands and fingers, which leads to the loss of fine motor skills. At later stages of the disease, extensor muscles in the lower limbs might also develop symptoms, most often in toe and ankle extensors. Even in later stages of the disease, symptoms in flexor or proximal muscles are rarely developed. Cardiomyopathy, dysphagia and respiratory failure are never observed (Welander 1951, Borg *et al.* 1998). Except for loss of ankle reflexes in later stages of the disease, tendon reflexes are mainly preserved throughout the disease (Udd, 2014). The loss of functionality in distal muscles may result in inability to perform manual tasks, such as threading a needle or opening doors with keys. Weakness in *tibialis anterior* and other muscles of the lower extremities causes difficulties in walking, causing a steppage gait (Welander, 1951). Although neuronal involvement has been suggested earlier (Borg *et al.* 1987), there is no actual evidence of it (Jaakko Sarparanta, personal communication).

The disease progresses slowly: patients are most often able to live normal lives and are rarely wheelchair bound as a result of the disease. The patient's life expectancy does not change following a diagnosis (Welander 1951).

Homozygotes for the mutation are rare, and more severely affected by the disease (Welander 1951). Homozygotes show symptoms earlier, at an average age of 30. In homozygotes both distal flexors and proximal muscles become involved within 5 to 10 years after onset. The course of the disease is more rapid and aggressive in these patients, who often lose their ability to walk during the progression of the disease, and eventually become wheelchair bound by the age of 50 (Welander 1951, Åhlberg *et al.* 1999).

As for most other muscular dystrophies, there is no pharmacological treatment for WDM, although patients may receive physiotherapy or be advised to increase strength through low to moderate intensity strength and aerobic training (Ansved, 2001).

5.2. HISTOPATHOLOGY

Histopathology of WDM muscle reveals a typical chronic myopathic muscular tissue with varying fiber size, split fibers, internal nuclei and fiber atrophy affecting both slow and fast fibers. Rimmed vacuoles are present to a variable degree in both normal-sized and atrophic fibers (Åhlberg *et al.* 1994).

Autophagic vacuoles can be observed by electron microscopy in WDM muscle (**figure 6**). Autophagic vacuoles are ultra-structural correlates to rimmed vacuoles. In association to them, tubulofilamentous inclusions are found in the sarcoplasm and occasionally in nuclei. Other reported abnormalities are fingerprint bodies, honeycomb structures, accumulations of Z-disc material, Z-disc streaming and changes in mitochondria (Borg *et al.* 1998).

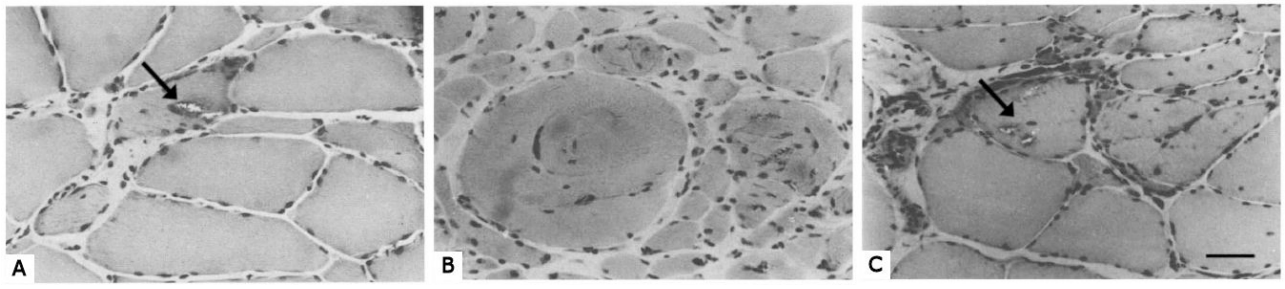

Figure 6. Histopathological changes in soleus (A and C) and *tibialis anterior* (B) in a patient with WDM. In all pictures atrophic fibers can be seen. In addition, rimmed vacuoles (shown by the arrows) can be seen in A and C. The bar in C represents 50µm. (Adapted from Åhlberg *et al.* 1994)

5.3. GENETICS

One common mutation is found in all known WDM cases in Sweden and Finland. It is a missense mutation c.1150G>A (RefSeq NM_022173.2) in a gene called *TIA1 cytotoxic granule-associated RNA-binding protein* (*TIA1*, also known as *T-cell intracellular antigen 1*, OMIM *603518) (Hackman *et al.* 2013). The mutation is located in a prion related domain in the 13th and last exon of the gene, and causes the change p.E384K (RefSeq NP_071505.2) in the third last amino acid in the protein product TIA1 (Hackman *et al.* 2013). Heterozygotes develop the typical symptoms for WDM, while homozygotes are affected more severely. The gene is thus described as semi-dominant (Welander 1957, Åhlberg *et al.* 1999, Hackman *et al.* 2013).

The disease has been recorded only in Sweden, Finland and Great Britain (one family) (Hackman *et al.* 2013). The prevalence of the disease is highest in Sweden, where 1/10,000 inhabitants are affected. The prevalence is higher in the central and northern parts of the country, where it can reach numbers as high as 1/70 (Åhlberg *et al.* 1999). In Finland, the estimated prevalence is >2/100,000 (Bjarne Udd, personal communication). The original appearance of the mutation has been estimated to date back circa 1050 years (Klar *et al.* 2013).

The causative mutation was found by targeted high-throughput and Sanger sequencing of the candidate WDM region by Hackman *et al.* 2013 and was further confirmed to be the pathogenic change by studying the stress response in cell cultures by immunofluorescence microscopy (Hackman *et al.* 2013).

TIA1

TIA1 cytotoxic granule-associated RNA-binding protein (OMIM *603518, RefSeq NM_022037), also known as T-cell intracellular antigen 1, is a cytoplasmic protein with multiple functions in splicing regulation, RNA metabolism and protein expression. It is associated with granule formation, and expressed in cytolytic lymphocytes (CTLs) and natural killer cells (Anderson *et al.* 1990). There are two splice isoforms of TIA1, which differ by a 33bp/11aa sequence that is excluded in exon 5 in TIA1b. There is no significant recorded difference in the functionality of the two transcript products (Hackman *et al.* 2013).

TIA1's domain structure as well as many of its functions is shared with its close homologue TIAL1 (TIA1-like, also known as TIAR, TIA1-related protein). TIA1 and TIAL1 are identical to ~80% in their amino acid sequences and ~50% in the prion-related domains (PRDs) (Kawakami *et al.* 1992).

The 13 exons of *TIA1* span over 46 kb of genomic DNA (Kawakami *et al.* 1994). The gene product, the TIA1 protein, contains three RNA-binding domains (RNA recognition motifs, RRM). These are followed by a C-terminal glutamine-rich PRD (Tian *et al.* 1991). The two splice variants occur as a result of alternative splicing. The longer isoform TIA1a (splice variant 2; RefSeq NP_071505) is 386 amino acids long, with a theoretical molecular weight of 43.0 kDa. In the shorter variant TIA1b (splice variant 1; RefSeq NP_071320), an exclusion of 11 amino acids is made in the exon 5 between the two first RRMs. The resulting protein is 375 amino acids long with a theoretical weight of 41.8 kDa (Tian *et al.* 1991, Kawakami *et al.* 1994). The TIA1 protein structure is visualized in **Fig. 7**, and the sequence including variants discussed in this thesis is found as **supplement 3**.

The localization of TIA1 in unstressed cells is primarily nuclear, although there is a constant exchange (shuttling) of the protein between the nucleus and the cytoplasm (Zhang *et al.* 2005). As a response to cellular stress, TIA1 is rapidly moved to the cytoplasm. The exact mechanism behind the relocation has not been reported, but it has been suggested that it would follow as a result from inactivation of nuclear import (Kedersha et al 1999).

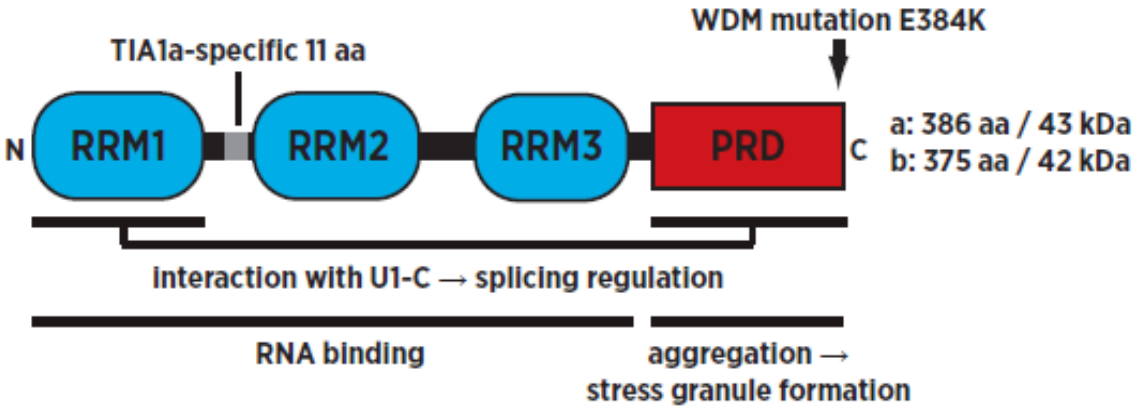

Figure 7. The TIA1 protein includes three different RNA-binding motifs (RRM1-3), which are followed by a glutamate-rich prion-related domain (PRD). The TIA1a-specific 11aa region, excluded in the TIA1b isoform, is shown in grey. Reprinted with permission from Jaakko Sarparanta.

The overexpression of TIA1 in cell cultures leads to stress granule formation (discussed under **6.1.1. Composition and mechanism of formation**), but also a simultaneous decrease in the expression of reporter genes. However, when the PRD domain is isolated and expressed in cells, TIA1 and TIAR binding cytoplasmic microaggregates are formed and a simultaneous increase in co-transfected reporter genes is noticed (Kedersha *et al.* 1999).

6. CELLULAR STRESS

In the event of a change in the cell's environment (stress), it has to either adapt to the new conditions or give up. Depending on the type of stress, the cell can thus either activate an apoptotic pathway leading to cell death, or induce survival mechanisms (Arimoto *et al.* 2008). The survival mechanisms often come at the cost of loss of functions that are not needed for survival. Changes in the environment that lead to the so called stress response include, but are not restricted to, changes in temperature, oxidative stress, ischemia, viral infections and UV radiation (Anderson and Kedersha 2008, Arimoto *et al.* 2008, Hofmann *et al.* 2012).

The eukaryotic cell has a variety of different proteins, which monitor changes in its environment. These proteins are also responsible of starting the stress response cascade when needed. Depending on what kind of stress the cell is exposed to, different pathways are activated as a response to the stress. The first reaction is often partial or complete translational arrest. The translational arrest saves the cell energy, which can then be reallocated and focused to processes that repair molecular damage caused by the stress (Anderson and Kedersha 2008). It has been shown that the decrease in protein synthesis that follows translational arrest is potentially selective, and that the synthesis of certain proteins increases under stressful conditions (Kawai *et al.* 2004). However, stress responses always lead to a reaction in the translational machinery and thus in the proteome of the cell (Anderson and Kedersha 2008).

In mammalian cells the environmental changes are monitored by five different eIF2α kinases: protein kinase R (PKR), pancreatic eIF2α-kinase (PERK), General control nonderepressible 2 (GCN2), heme-regulated eIF2α kinase (HRI), and Z-DNA. These kinases all react to mainly different, but partially the same changes, as indicated in **Table 3**. The kinases' task is to start the cascade that leads to translational inhibition. The mechanism is discussed under section **6.2. Composition and mechanism of formation**.

Table 3. The five kinases in charge of inducing the stress response. ER = endoplasmic reticulum.

Kinase	Activated by	Reference
PKR	Viral infection, heat shock, UV radiation	Srivastava *et al.* 1998
PERK	Accumulation of unfolded proteins in ER	Harding *et al.* 1998, Harding *et al.* 2000, Hoffman *et al. 2000*
GCN2	Starvation (decreased amount of free amino acids)	Wek *et al. 1995*
HRI	Oxidative stress	McEwen *et al. 2005*
Z-DNA	Immunological response to viral infection	Wek *et al.* 1995

6.1. STRESS GRANULES

Stress granules (SGs) are functional by-products of mRNA metabolism observed in yeast, plant and metazoan cells. SGs are formed by stalled translation pre-initiation complexes that aggregate with different proteins in the event of stressful conditions (Anderson and Kedersha 2002).

SGs are observed in cells that have been exposed to environmental changes that induce the cell's survival mechanisms – stress (**Fig. 8**). In the event of stress, eukaryotic cells reprogram their translational machinery. By reducing the global translation and thus avoiding translating unnecessary proteins, cells reallocate their resources in order to selectively express proteins needed for viability and cellular survival under the new or changing conditions (Kedersha *et al.* 2005, Hofmann *et al.* 2012).

SGs are highly dynamic, in contrast to static ribonucleoprotein (RNP) aggregates. There is a constant exchange of proteins and mRNA between SGs and the cytosol, often referred to as shuttling. Fluorescence recovery after photobleaching (FRAP) studies have shown, that protein components and reporter mRNAs may reside in SGs from seconds to minutes. One of the most mobile protein components is TIA1, which shows a ~90% fluorescence recovery within 10 seconds of bleaching (Kedersha *et al.* 2000, Hackman *et al.* 2013).

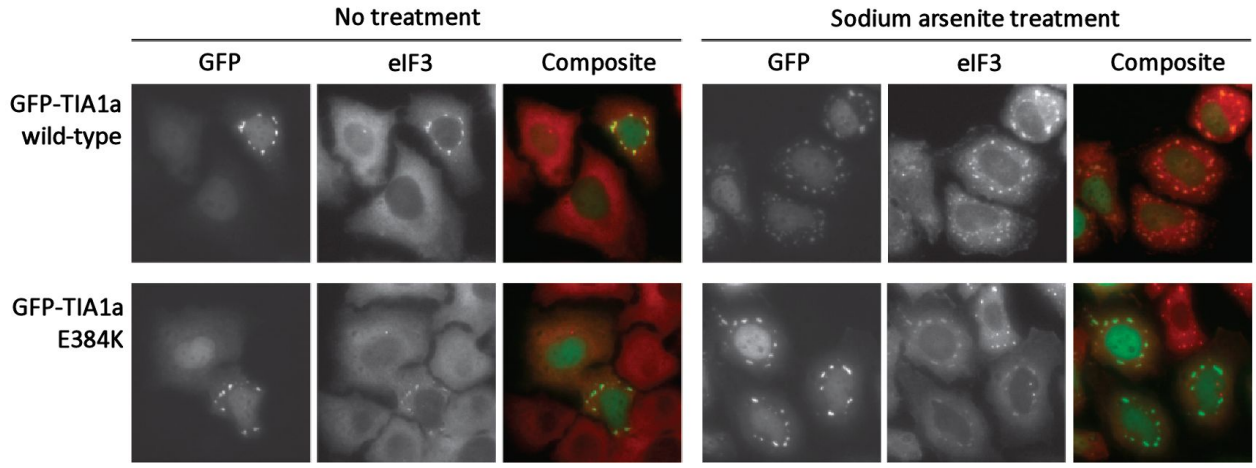

Figure 8. Immunofluorescence image of HeLa cells transfected with green fluorescent protein (GFP) tagged TIA1 constructs. Here, the TIA1a wild type and p.E384K mutation without stress inducing treatment are shown side-by-side with cells that have been treated with sodium arsenite to induce a stress response. TIA1a is seen as clear green granules around the nucleus. The arsenite treated cells show a significant increase in stress granule amount compared to the non-treated cells (Adapted from Hackman *et al.* 2013).

6.1.1. COMPOSITION AND MECHANISM OF FORMATION

A correct regulation of gene expression is dependent on a meticulous control of the mRNA translation, localization and degradation, especially in situations such as during stress or embryogenesis (Buchan *et al.* 2013).

SGs are formed by stalled 48S-preinitiation complexes, which form cytoplasmic complexes (granules) with different proteins (Anderson and Kedersha 2008). The main components beyond the stalled preinitiation complexes are the early initiation factors eIF4E, eIF3, eIF4A, eIFG and poly-A-binding protein 1 (PABP). The granules also contain RNA-binding proteins that play a role in the regulation of mRNA translation and decay, as well as other proteins involved in the mRNA metabolism. SGs have also been found to contain proteins related to the regulation of cell signaling pathways (e.g. TRAF2; Hofmann *et al.* 2012, Kim *et al.* 2005).

The composition of the granules varies both over time and depending on which kind of stress induces their assembly (Anderson and Kedersha 2008). Far over one hundred different protein coding genes have been found to play a role in the composition of stress granules and the regulation of their formation (Buchan *et al.* 2013). The metabolism of mRNA can thus be assumed to depend on a largely unknown, vast and intricate network of different kinds of interactions between different genes and proteins (Buchan *et al.* 2013). Some of the identified proteins in association to SGs are shown in **Table 4**.

Table 4. SG-associated proteins (adapted from Anderson and Kedersha, 2008)

Protein	Relevant binding partners	Nucleates SGs?	Known functions
Ago2	FXR1, RISC	Yes	RNAi slicer
APOBEC3G	?	No	Antiviral response
Ataxin-2	PABP-1	No	Translation
Caprin-1	G3BP	Yes	Cell growth
CPEB	RCK, eIF4E, FXR1	Yes	mRNA silencing
DIS1	eIF3h	Yes	Unknown
eIF3	40S, eIF4G	?	Translation
eIF4E	CPEB, smg, eIF4G, 4ET	No	Translation
eIF4G	eIF4E, eIF3, PABP-1	?	Translation
FAST	TIA-1	Yes	Translation
FMRP and FXR1	Ago2, RISC	Yes	Translation
FBP and KSRP	TIA-1	No	RNA decay
G3BP	Caprin	Yes	Ras signalling
HuR	?	No	RNA stability
IP5K	?	Yes	Signaling
Lin28	?	?	Development
LINE1 ORF1p	?	Yes	Transposon
MLN51	Exon junction	No	Splicing
PABP-1	eIF4G, eIF3, ataxin-2	No	Translation, stability
DDX6 (p54)	HedIs (GE-1), TTP	Yes	mRNA decay
Plakophilin	G3BP FXR1	No	Adhesion
PMR1	TIA1	No	mRNA decay
Pumilio 2	?	Yes	mRNA silencing
Rap55	?	?	mRNA silencing
Rpb4	?	?	Transcription
SRC3	TIA1	No	Transcription
Staufen	?	No	mRNA silencing
SMN	SMN complex	Yes	RNP assembly
TIA1 and TIAR	FAST, SRC3, PMR1, FBP	Yes	mRNA silencing
TRAF2	eIF4G	No	Signaling
TTP and BRF-1	DDX6 (p54)	Yes	mRNA decay
YB-1	?	?	Cold-shock RNA binding protein
ZBP1	?	No	Localization

Stress granule assembly is known to happen according to two different principles:

1) Translational silencing, which leads to the presence of non-translating RNA, and
2) dimerization or aggregation of mRNP-binding proteins

The SG assembly and stress-induced translational arrest is known to be initiated by phosphorylation of translation initiation factor eIF2α (Kedersha *et al.* 2005), which is mediated by five stress monitoring kinases (HRI, PERK, GCN2, PKR and Z-DNA kinase) in mammals (Anderson and Kedersha, 2008). In normal cases, eIF2α brings the translational initiator $tRNAi^{Met}$ to the 40S ribosomal unit (Holick and Sonenberg, 2005).

Once phosphorylated, eIF2α can no longer dissociate from eIF2B, its guanosine diphosphatase (GDP) exchange factor. This in turn prevents recharging of the eIF2α-GTP-tRNAi^{Met} ternary complex, which is needed to initiate protein translation. mRNP-binding proteins that are present in the cytosol (such as TIA1) are then bound to the stalled translation initiation complex. Due to the ability of the protein to bind both RNA and protein, the stalled translation initiation complexes bind with each other and form complexes (Anderson and Kedersha 2008). The phosphorylation of eIF2α thus leads to stalled translation pre-initiation complexes that aggregate in the cytosol: SGs (Kedersha *et al.* 1999). This mechanism is shown in **Fig. 9.**

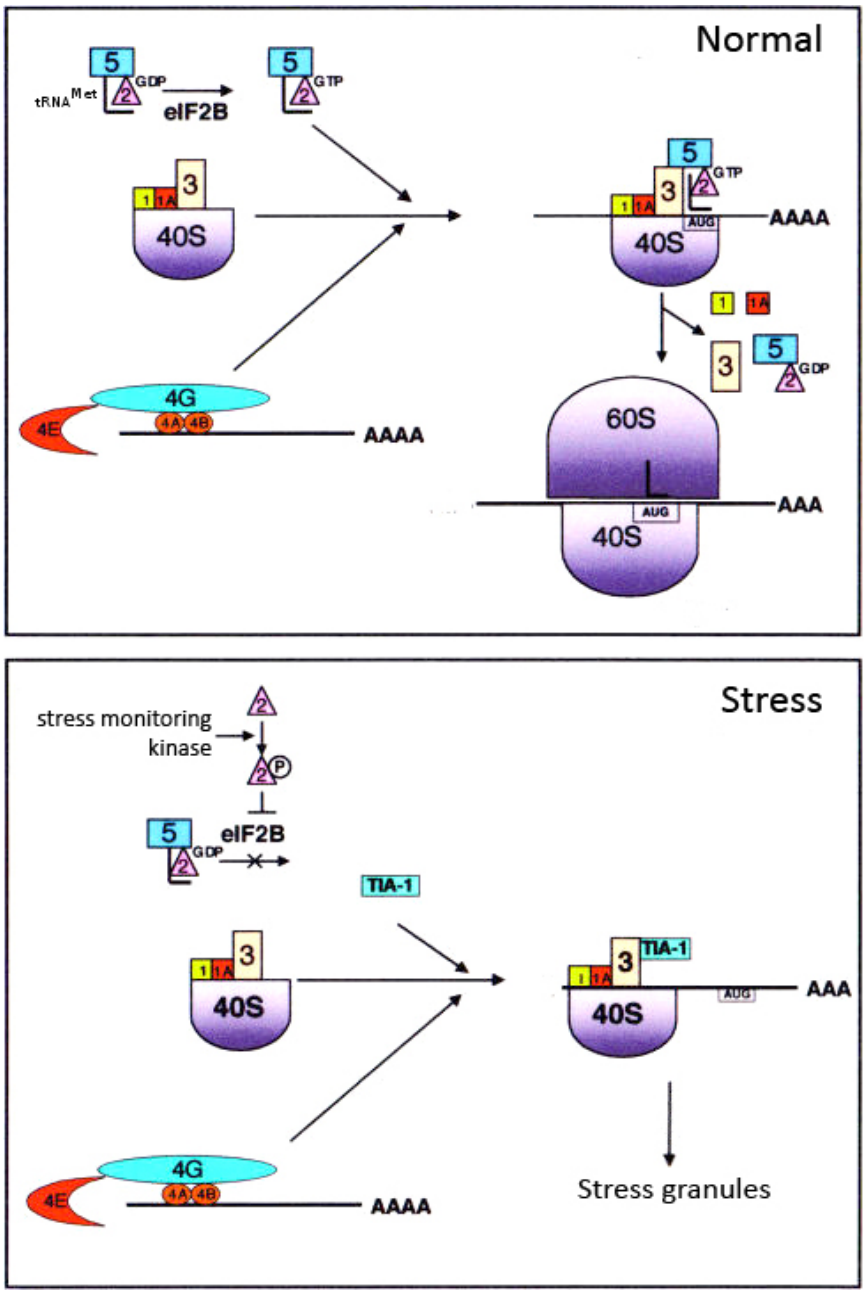

Legend:

1-5: Early initiation factors (eIFs)
40S: The small ribosomal subunit
60S: The large ribosomal subunit
AUG: Start codon
GDP: Guanosine diphosphate
GTP: Guanosine triphosphate
TIA1: TIA1 protein

tRNA Met depicted as an L-formed strand
mRNA depicted as long strand with a poly-A tail

Figure 9. The mechanism of stress granule formation. In normal cells eIF2α-GDP is phosphorylated to eIF2α-GTP. A translation complex is then built by eIF2α-GTP, the ribosomal 40S subunit initiation factors included and the $tRNAi^{Met}$ translation initiator. The initiation factors leave the complex when bound, and the ribosomal 60S subunit can bind to the complex and the translation is initiated. In the case of stress, a stress monitoring kinase (PKR in the example) responds to the environmental stress by phosphorylating eIF2α, which prevents it from dissociating from the GDP exchange factor eIF2B. This allows TIA1 to bind to the translation initiation complex. TIA1 inhibits the initiation factors from dissociating the complex, and thus the ribosomal 60S subunit is unable to bind to the complex. TIA1 subsequently aggregates with itself in other stalled translation initiation complexes and stress granules are formed. (Adapted from Anderson and Kedersha, 2008)

The common components included in all stress granules are the stalled initiation complexes, that are still bound to the mRNA and that have been moved from the degraded polysomes to the granules. The composition of stress granules does however vary to some degree depending on a number of factors, such as what kind of stress induces their formation, in which kind of cell they are formed and also how long the response has lasted (Anderson and Kedersha 2008).

Furthermore, the different components included in stress granules are divided into a couple of categories. Stress granules can contain a number of different mRNA binding proteins, which have roles in translational silencing and mRNA stability. These proteins can function as markers for stress granules, but are not necessarily present in all stress granules. An example of such a protein is TIA1 (Anderson and Kedersha 2008).

Another group of stress granule related proteins are the proteins that regulate the RNA metabolism in other ways than controlling the translation or degradation of mRNA. Proteins involved in splicing, RNA modifications, and RNA localization belong to this group. These proteins have been noticed to cause stress granule formation when over expressed in cell cultures (Anderson and Kedersha 2008). TIA1 represents this group of proteins as well (Gilks *et al.* 2004).

It has been proposed, that the formation of stress granules is also at least somewhat dependent of the cytoplasmic skeleton. Cells exposed to both SG inducing and microtubule-depolymerizing treatments (arsenite and vinblastine respectively) produce no SGs, whilst control cells treated with only arsenite assemble stress granules as expected. This suggests the involvement of microtubule as a facilitator of the stress granule assembly (Ivanov *et al.* 2003).

If the environmental factors return towards a more favorable situation for the cell and the stress response in silenced, the stress granules are dissolved. In cell cultures the granules are degraded in minutes, when optimal cell conditions are restored after a stress-inducing treatment. Before they are degraded, they seem to accumulate into fewer but larger granules, which are then rapidly degraded (Buchan *et al.* 2013). It is still partly unknown on what basis the cell determines how the stress granule components will be degraded. To some extent the translation is resumed from the point at which it was stopped in the translation initiation complexes, but some complexes are degraded to their very basic building blocks (Buchan *et al.* 2013).

It has furthermore been shown that cells dispose of SGs to some degree by autophagy. The granules are targeted to vacuoles, which degrade them (Buchan *et al.* 2013).

6.1.2. THE ROLE AND IMPORTANCE OF TIA1 AND STRESS GRANULES

The WDM causing mutation was studied by transfecting HeLa cells (derived from human cervical cancer) with a GFP-tagged TIA1-protein (Hackman *et al.* 2013), as it causes the formation of stress granules when over expressed (Gilks *et al.* 2004). The cells were studied with immunofluorescence microscopy. Cells that were transfected with the WDM-mutation p.E384K showed a 10-20% increase in both stress granule size and number (Hackman *et al.* 2013).

The mutated glutamate residue is highly conserved in all tetrapodes. In addition, it is located in the protein's PRD-domain, which plays a role in its ability to self-aggregate (Hackman *et al.* 2013).

Environmental factors have been proposed to affect the development of disease in Welander Distal Myopathy. Hofmann *et al.* observed an increased number of stress granules in several mammalian cell lines treated with cold shock compared to cells kept in 30°C, using eIF3B as a marker (Hofmann *et al.* 2012).

Their findings are of interest due to the nature of WDM; the symptoms start in the distal muscles of the extremities, the temperature of which is often significantly lower compared to the body's core temperature. Furthermore the disease is encountered only in countries with relatively cold climates, which could hypothetically be caused by the fact that people living in warmer climates do not express symptoms despite harboring the causative mutation, due to not being exposed to cold climates.

In a number of patients with WDM-like symptoms lacking the c.1150G>A mutation, a c.1070A>G change has been found (Hackman *et al.* unpublished). This c.1070A>G change has earlier been reported as a polymorphism (rs116621885), and it causes an amino acid change from asparagine to serine in the 357th amino acid (p.N357S). The change in question is located 80 base pairs upstream from the WDM-causing mutation in the same PRD. Therefore, the p.N357S-change could theoretically affect the predisposition to increased formation of stress granules. For the amino acid sequences for the proteins encoded by the different *TIA1* variants, refer to **supplement 3**.

As the case with *TIA1* and WDM shows, stress granules are potential pathological indicators to other degenerative diseases as well. Mutations in different stress granule related proteins lead to different kinds of changes in stress granule size, number and dynamics. Besides being pathological indicators, stress granules have also been suggested to contribute to the actual pathogenesis of diseases (Anderson and Kedersha 2008).

The Fragile X syndrome is caused by mutations in the gene coding for fragile X mental retardation protein (FMRP). Patients with Fragile X have immature dendritic spines as a probable result of malfunctioning translational machinery. FMRP is an RNA-binding protein, and plays a role in the synthesis of synaptic proteins. It has been suggested that a malfunctioning FMRP protein could contribute to the deficient development of the synaptic dendrites, and in addition cause accumulation of SGs. In studies, FMRP is also seen as a component of the mRNA granules (Antar *et al.* 2005).

Radiation therapy of cancer tumors causes the tumor cells to express a protein called hypoxia inducible factor 1 (HIF-1). HIF-1 induces the production of mRNA that codes for endothelial survival factors. Endothelial cell damage is a strong indicator of the efficiency of the radiation therapy. The transcripts that HIF-1 induces can though be silenced by stress granules, which causes a larger amount of damage on the endothelial cells and thus reinforces the efficiency of the radiation therapy (Moeller, 2004).

7. AIMS OF THE STUDY

The study can be divided into two parts:

I) SUBPROJECT I: SNP p.N357S

The objective of the experiment was to explore the effects of the p.N357S-change in TIA1 and evaluate the possibility of it being a pathogenic mutation. The p.N357S change was induced in pEGFP-TIA1 constructs by mutagenic PCR, transfected into and expressed in HeLa (human cervical cancer) and 293T (human embryonic kidney) cells. The cells were then studied by the same methods as used to confirm the pathogenesis of the p.E384K WDM-causing mutation: expression and solubility tests, CellInsight spot count analysis and FRAP (Hackman *et al.* 2013).

The hypothesis was that p.N357S TIA1 would behave differently from the wild-type, and the expectation was to see similar changes as with the Welander causing mutation p.E384K, as the phenotype is very similar. It was thus expected, that the p.N357S transfected cells would display a larger amount of stress granule compared to the cells transfected with the wild type gene. In addition, it was expected for the p.N357S transfected cells to express stress granules that, alike to p.E384K transfected cells, recover slower in FRAP studies.

II) SUBPROJECT II: THE EFFECT OF COLD SHOCK ON STRESS GRANULES

The objective of the experiment was to test whether HeLa cells transfected with pEGFP-TIA1 p.E384K constructs expressed different levels of stress granules compared to their wild-type counterparts when treated with cold shock, and, ultimately, whether cold shock could induce a pathological amount of stress granules in the cells. HeLa cells were transfected with the selected constructs, treated with cold shock and imaged and analyzed using CellInsight platform.

The hypothesis was that p.E384K TIA1 would show an increased amount of stress granules as compared to the wild-type due to the SNPs previously shown behavior in arsenite treated cell cultures (Hackman *et al.* 2013).

8. MATERIAL AND METHODS

8.1. CELL CULTURE CONDITIONS AND METHODS (I & II)

HeLa cells (ATCC, Manassas, VA, USA) were cultured at 37ºC, 5% CO_2 in Dulbecco modified Eagle medium (Life Technologies Inc Gibco/Brl Division, Grand Island, NY, USA) with 10% fetal calf serum, GlutaMAX (Invitrogen/Life Technologies, Carlsbad, CA, USA) and penicillin/streptomycin. Transfections were done with FuGENE 6 (Promega Corporation, Madison, WI, USA), according to the manufacturer's instructions.

The pEGFP-TIA1a and b wild-type and p.E384K constructs used in transfections were received from Jaakko Sarparanta, and were identical to those used in the Hackman et al 2013 paper. The pEGFP-TIA1a and b p.N357S constructs were created by mutagenic PCR in the pEGFP-TIA1 wild-type constructs, the process of which is described under section **8.5. Creation of pEGFP-TIA1 p.N357S plasmid**.

8.2. CELLINSIGHT HIGH CONTENT IMAGE ANALYSIS (I & II)

HeLa cells were seeded on 24-well plates at a density of 75k cells/well. The cells were then transfected with GFP-TIA1 constructs. Cells were treated with 500 μM sodium arsenite (Thermo Fisher Scientific, Waltham, MA, USA) or control medium 18h after transfection for 45 minutes, after which they were fixed with 4% paraformaldehyde (PFA)/phosphate-buffered saline (PBS). The cells were permeabilized with 0.2% Triton X-100 in PBS and stained with Hoechst to label the nuclei.

The cells were imaged by using the CellInsight instrument (Thermo Fisher Scientific). Per well, 100 images were captured using a 10×/NA 0.3 objective and fixed exposure times through two channels. The images were analyzed using the automated image analysis software SpotDetector V4 Bio Application in vHCS Scan 6.2.3 (Thermo Fisher Scientific).

Based on mean fluorescence intensity of the entire cell, cells expressing moderate levels of TIA1 were selected for further analysis. The fluorescent spots (stress granules) that fulfilled pre-determined criteria of size, shape and intensity from a selected region of interest surrounding the nucleus were analyzed (**Fig. 10**). The results were normalized to the mean of the control wells (untreated wild-type) on the same plate.

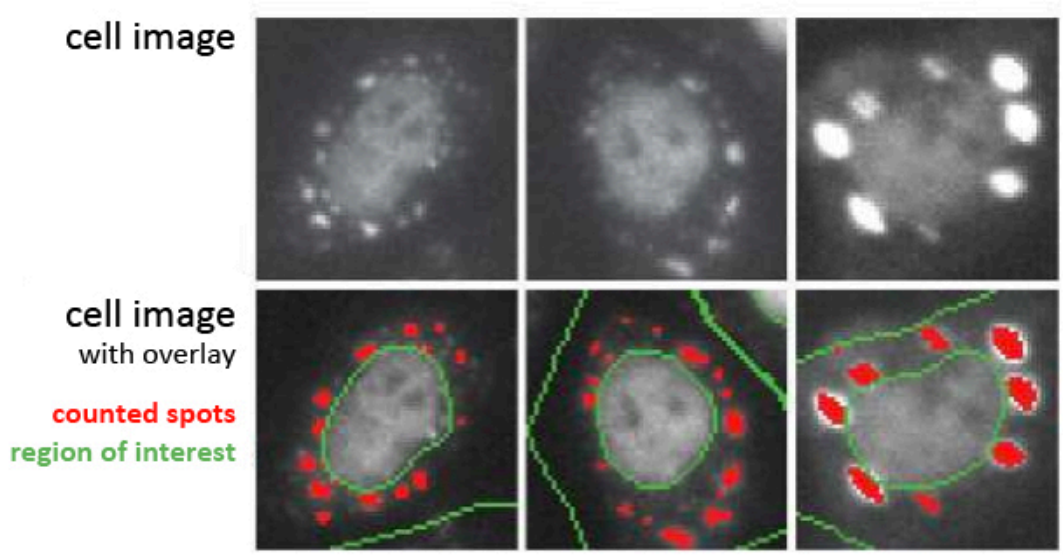

Figure 10. Demo of CellInsight analysis principle, showing the region of interest (ROI) boundaries around the nuclei and the cells in green and the counted spots in red. (Adapted from Hackman *et al.* 2013)

8.3. IMAGE PROCESSING AND ANALYSIS (I & II)

Images were processed and analyzed using a variety of different software: Adobe Photoshop CS4 Extended 11.0.2 (Adobe Systems Inc., San Jose, CA, USA), GNU Image Manipulation Program (various versions, http://www.gimp.org), ImageJ (various versions, US National Institutes of Health, Bethesda, MD, USA), ImageStudioLite 5.0.21 (LI-COR Biosciences, Lincoln, NE, USA) LSM 510 Meta 3.2 software (Carl Zeiss MicroImaging GmbH, Göttingen, Germany), Odyssey Infrared Laser Imaging System (LI-COR Biosciences), and vHCS Scan 6.2.3 software (Thermo Fisher Scientific).

8.4. STATISTICAL ANALYSIS METHODS (I & II)

Statistical analyzes for CellInsight and FRAP data were performed in Microsoft Excel 14.1.4. (Microsoft, Redmond, WA, USA) and IBM SPSS Statistics (various versions, International Business Machines Corporation, Armonk, NY, USA).

The spot count data for each group was pooled and normalized according to the mean of untreated wild-type relative spot counts. Significance levels (p values) of the spot count differences were determined according to the 2-tailed Mann-Whitney U-test or an independent sample T-test where the former could not be implemented. The methods are used to determine the significance of the difference between two independent data groups that consist of ordinal responses.

8.5. CREATION OF EGFP-TIA1 p.N357S PLASMID (I)

A mutagenic PCR was executed using existing pEGFP-TIA1a and pEGFP-TIA1b plasmids (Hackman *et al.* 2013) as templates.

The mutagenic primers were designed manually by determining the position of the wanted point mutation in the plasmid using the sequence of the gene and the plasmid (Ensemble and Invitrogen, respectively). The forward primer included a mismatch nucleotide at the wanted position to induce the mutation. The melting temperatures of the primers were matched using the Tm calculator of Life Technologies. The primers were ordered from Sigma Aldrich (St. Louis, MO, USA).

The mutagenic PCR was executed using Phusion™ High-Fidelity DNA Polymerase (Thermo Scientific). For the plasmid map and PCR conditions including primer sequences, see **supplement 1 and 2** respectively.

The PCR products were confirmed by running them in a 0.8% agarose gel (110 V, 45 min), purified using NucleoSpin Plasmid (Machery-Nagel, protocol 5.5. Support protocol Plasmid (NoLid) and NucleoSpin Plasmid Quick Pure Plasmid Clean-up and 5.1. Isolation of high-copy plasmids from *E. coli*, from step 5 onward). Purified PCR products were ligated with Quick T4 DNA Ligase (New England BioLabs, Ipswich, MA, USA). The reaction mix is shown in **Table 4**. 2,5 µl of ligation mix per construct was transformed into 25 µl of OneShot TOP10 Chemically Competent *E. coli* cells (Invitrogen/Life Technologies) according to the corresponding protocol, and plated on kanamycin containing LB agar plates.

Table 4. Ligation reaction mix for mutagenic pEGFP-TIA1 p.N357S PCR products

Reagent	Amount/reaction
PCR product	1 µl
Water	9 µl
Quick Ligase Buffer (2x)	10 µl
Quick T4 DNA Ligase	1 µl
Σ	21 µl

Pure liquid cultures were made from the transformant colonies, from which plasmids were extracted using Fermentas NucleoSpin (protocol for high-copy plasmid preps from *E. coli*). The samples were then digested with EcoRI Fast-Digest (Fermentas, Vilnius, Lithuania) for 10 min at 37ºC and run in a 0.8% agarose gel (120 V, 35 min) to confirm successful ligation. Confirmation of successful mutagenesis was done by sequencing (FIMM).

Successfully mutagenized pEGFP-TIA1a and pEGFP-TIA1b samples along with the original wild type pEGFP-TIA1a and pEGFP-TIA1b constructs were digested with BamHI and HindIII (New England BioLabs) for 15 min at 37ºC and 20 min at 80ºC for HindIII inactivation. The samples were then run in a 0.8% agarose gel (110 V, 35 min). The bands of the mutagenic inserts and the wild type vector were extracted from the gel using a GeneJet Gel Extraction Kit (Fermentas).

The purified samples were ligated with Quick T4 DNA Ligase (New England BioLabs) and transformed into 5α chemically competent *E. coli* (New England BioLabs). Ligation of insert was confirmed by restriction analysis with BamHI and HindIII (New England BioLabs) as above and the samples were sequenced (FIMM) to ensure correct sequence (see **supplement 4**).

Midi-preps were made of all correct transformants using a HiSpeed Plasmid Midi Kit (Qiagen, Hilden, Germany). The yield and purity was checked with spectrophotometry at wavelength 260 nm and 280 nm using NanoDrop 1000 3.6.2. (Thermo Scientific)

8.6. INDUCTION OF STRESS GRANULES BY ARSENITE TREATMENT (I)

Stress granule assembly was induced by generating oxidative stress conditions by treating cultured HeLa cells with 500 μM sodium arsenite in normal media for 45 minutes before cell fixation. For control cells, the old media was changed for fresh media but no further steps were taken.

8.7. EXPRESSION AND SOLUBILITY TESTS (I)

The expression and solubility tests were performed to assess whether the mutation would affect the expression or the solubility of the protein. It has earlier been concluded that the p.E384K mutation does not affect these features (Hackman *et al.* 2013), but it was included in the analysis nonetheless.

The tests were performed in HeLa and 293T cells. HeLa cells were also used for the CellInsight stress granule quantification analysis and FRAP. In addition, this worked as a transfection test of the produced constructs. 293T cells are significantly more efficient than HeLa cells at over-expressing transfected proteins and thus possible differences in expression can be more prominent in them. Due to these differences in qualities between the two cell lines, the test in HeLa was regarded a transfection and expression test, whilst the test in 293T was used to assess protein features.

Both cell lines were transfected with isoforms a and b of wild-type, p.E384K and p.N357S *TIA1*. The same protocol was used for both cell lines.

The cells were seeded on 2×6–well plates and transfected with GFP-tagged TIA1 constructs. The cells were allowed to express the proteins for 24 h. The cells were then washed with PBS, resuspended in 1 ml of PBS and transferred to eppendorf tubes. The cells were pelleted (10 min, 500 g), the supernatant was removed and the pellet was chilled on ice. The pellet was then resuspended in radioimmunoprecipitation assay (RIPA) buffer (50 mM Tris-HCl pH 8.0, 150 mM NaCl, 1% Triton X-100, 0.1% SDS, 0.5% sodium deoxycholate) containing 1:100 protease inhibitor (Halt^{TM} Protease Inhibitor Cocktail, Thermo Fisher Scientific) and incubated on ice for 15min. The sample was vortexed twice during the incubation.

The cells were pelleted (15 min, 13000 g) and a 10 µl sample was taken from the supernatant. 130 µl of 2× SDS Sample Buffer and 3.3 µl of β-mercaptoethanol was added.

The pellet was washed and resuspended in RIPA buffer (without protease inhibitor) and centrifuged (15 min, 13000 g). The supernatant was removed and 100 µl of 1× SDS Sample Buffer and 1.2 µl β-mercaptoethanol was added. The samples were incubated at 65°C for 30 min. Both the supernatant and the pellet samples were then boiled for 5 min at 95°C.

The samples were run in a sodium dodecyl sulfate-polyacrylamide gel electrophoresis (SDS-PAGE) (Bio-Rad) and blotted to a nitrocellulose membrane using Bio-Rad's Trans-Blot Turbo Blotting System. The membrane was blocked with 5% milk in PBS for 1 h at RT, and then incubated in 1% milk in PBS with 0.1% Tween-20 (PBST) and primary antibodies over night. The antibodies used were against GFP (FL) Rabbit polyclonal IgG (SC8334, Santa Cruz Biotechnology, Inc., Santa Cruz, CA, USA) and α-tubulin (AB 6160, YL1/2, Abcam plc, Cambridge, UK).

The membrane was washed with PBST buffer repeatedly over the course of 1 h to ensure removal of all non-bound primary antibodies. The membrane was then incubated in 1% milk with 0.1% Tween-20, 0.01% SDS and secondary antibodies for 1 h at RT. The secondary antibodies used were Alexa Fluor 680 anti-rat IgG (H+L) (A21096, Invitrogen) and IRDye 800CW goat anti-Rabbit IgG (H+L) (926-32211, Li-COR Biosciences, Lincoln, NE, USA). The membrane was then washed with PBST and finally with PBS and scanned using Odyssey Infrared Laser Imaging System (LI-COR Biosciences).

The membranes of the expression and solubility tests were analyzed with ImageJ and Microsoft Excel. A 30×30 pixel or 130×30 pixel square was drawn around each band for HeLa and 293T samples respectively. The returned intensity curve was measured by manually selecting a horizontal baseline for the curve, excluding possible background, as objectively as possible. The area under the curve was then measured, returning a value reflecting the intensity of the band.

The values were normalized by issuing a factor to each sample based on the intensity of the tubulin band as compared to the mean of all tubulin bands. The bands representing GFP were then multiplied by this factor and then compared with the normalized tubulin value.

The values were assembled in Microsoft Excel and *p* values were calculated by a independent samples T-test in SPSS.

8.8. FLUORESCENCE RECOVERY AFTER PHOTOBLEACHING (I)

GFP-TIA1a wild-type, p.E384K and p.N357S transfected HeLa cells were seeded on Lab-Tek II chambered cover slides (Nunc A/S, Roskilde, Denmark) in phenol-red-free medium. Cells were treated with 500 μM sodium arsenite or control medium 18h after transfection to induce stress granule formation. The cells were analyzed with FRAP at 37ºC, 5% CO_2 within 55 minutes after stress induction.

The FRAP measurements were performed with an LSM510 Duo confocal microscope equipped with an LD C-Apochromat 40×/NA 1.1 water immersion objective (Carl Zeiss Micro-Imaging) The instrument zoom factor was set to 20× and the frame size to 90×90 pixels. Inside this frame, a circular target of 8 pixels (equivalent of 1 μm) was selected and centered on a stress granule. The selected area was bleached with three laser lines (405 nm, 458 nm, 488 nm) by point bleaching. For each analyzed granule, a time series of 40 frames was captured – 5 frames were captured before bleaching and 35 after. The frames were taken with maximum acquisition speed at intervals of 250 ms.

The resulting images were analyzed in ImageJ (version 1.48, http://imagej.nih.gov/ij/). The mean fluorescence intensity was measured from three regions: inside the targeted FRAP region, a reference region from a non-bleached stress granule, and a reference region from outside the cell. Image series where stress granules moved partly or completely away from the measurement or

bleaching regions, or where the bleaching caused an obvious intensity drop in the non-targeted stress granule were discarded. In total, 30 granules were analyzed of GFP-TIA1a p.E384K transfected cells, 27 of wild-type transfected cells and 36 of p.N357S transfected cells.

The returned value for imaging background was subtracted from the measured fluorescence intensity value of the region of interest. This was done for each frame separately. The values for each analyzed granule were normalized to the initial fluorescence intensity (frame 1) of the series to make the values comparable. The values for all wild-type, p.E384K and p.N357S samples were then plotted together, and averaged to build a visualization of the data.

Significance values were calculated in SPSS using the 2-tailed Mann-Whitney *U* test.

8.9. COLD SHOCK (II)

Cold shock was induced 18h after transfection by transferring plates seeded with both GFP-TIA1a wild type and p.E384K (cultured in CO_2-independend media by Invitrogen/Life Technologies) to the cold room at 9.0 –12.5°C for 4–8 h. The plates were placed directly on lead blocks pre-cooled to the cold room temperature and covered as to minimize temperature fluctuation and changes in lighting during the cold shock. The temperature was monitored during the cold shock treatment both inside and outside the insulation.

9. RESULTS AND DISCUSSION

9.1. SUBPROJECT I: SNP p.N357S

9.1.1. EXPRESSION AND SOLUBILITY TESTS

The intensity of the GFP-tagged bands in the blots (shown in green) for HeLa samples (**Fig. 11**) and 293T samples (**Fig. 12**) was measured, normalized to the mean value of tubulin (shown in red on the blots) and compared against each other. No significant difference between the constructs was recorded.

As seen from the HeLa blot (**Fig. 11**) the construct is transfectable and the HeLa cells can express the GFP-tagged TIA1 protein, as it is clearly visible in the blot. Furthermore, as expected, protein over-expression in 293T cells is significantly more effective than in HeLa cells, which is clearly seen when comparing the western blots in **Fig. 12** to those in **Fig. 11**.

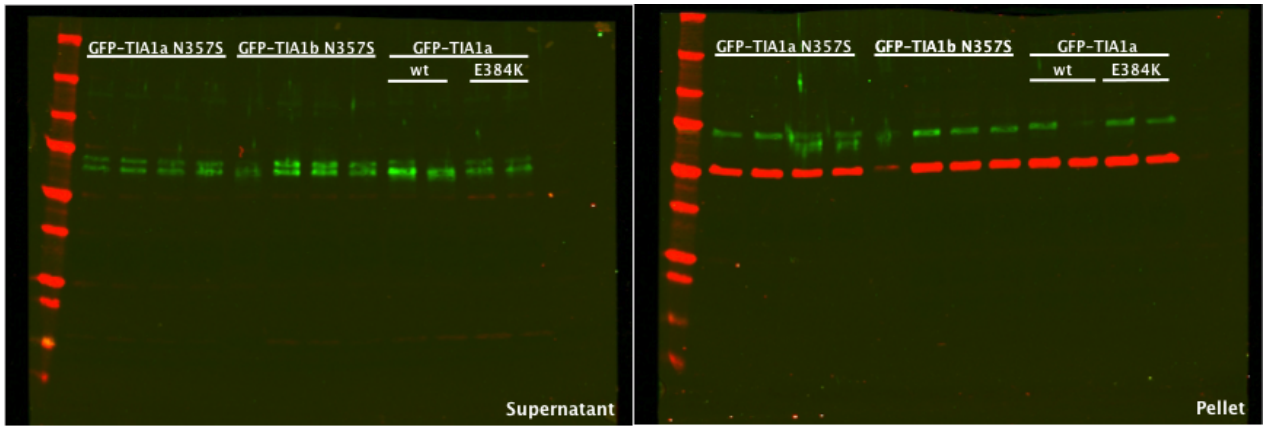

Figure 11. Expression and solubility test of TIA1 isoforms a and b wild-type, p.E384K and p.N357S in HeLa cells, showing supernatant on the left and pellets on the right. The first sample of GFP-TIA1b p.N357S and the second sample of GFP-TIA1a wt were excluded from the analysis due to pipetting errors. Tubulin shown in red, GFP in green.

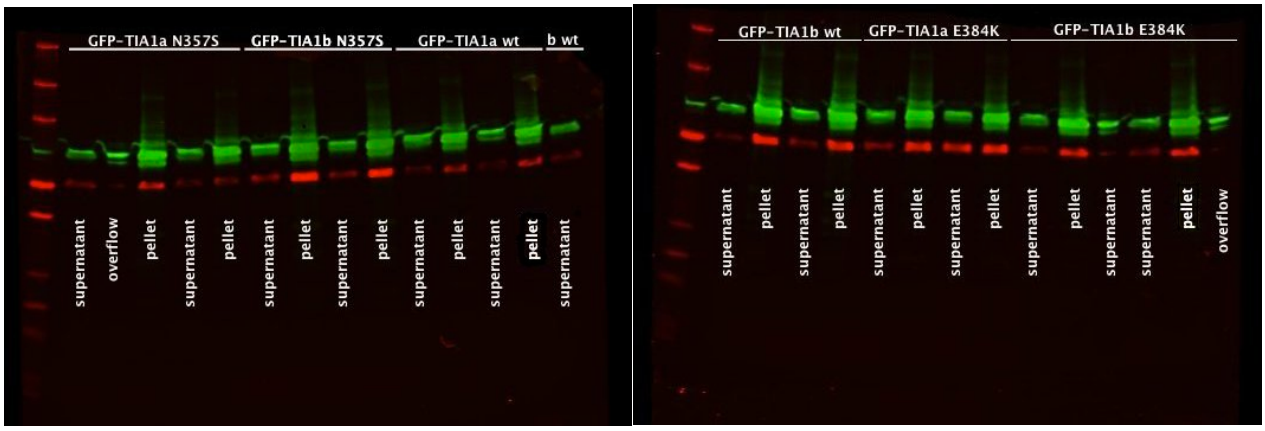

Figure 12. Expression and solubility test of TIA1 isoforms a and b wild-type, p.E384K and p.N357S in 293T cells. Sample GFP-TIA1b wt in the left picture and the third supernatant sample of GFP-TIA1b p.E384K, along with wells showing overflow material were excluded from the analysis due to pipetting errors. Tubulin shown in red, GFP in green.

As seen in **Fig. 11 and 12**, the expression and solubility tests returned similar results for the tests on both used cell lines, indicating no obvious difference between the samples within the sets. Based on this, the assumption was made that the amino acid change from asparagine to serine does not cause a significant change in TIA1 solubility. However, a functional difference in protein mechanisms cannot be ruled out by the confirmation of similar expression and solubility levels.

9.1.2. CELLINSIGHT HIGH CONTENT IMAGE ANALYSIS (I)

Fig. 13 shows an example of the images taken with the CellInsight platform. The used Hoechst-dye is targeted solely to the nuclei, as Hoechst targets DNA. The GFP-tagged TIA1 is shown in both the nuclei and the stress granules, which are seen as clear spots in the cytosol, often in close proximity to the nucleus. It is to be noted that the TIA1 in the cytosol is seen as distinct aggregates. The nucleus, however, shows a relatively even GFP-signal, indicating that TIA1 in the nucleus is not aggregated.

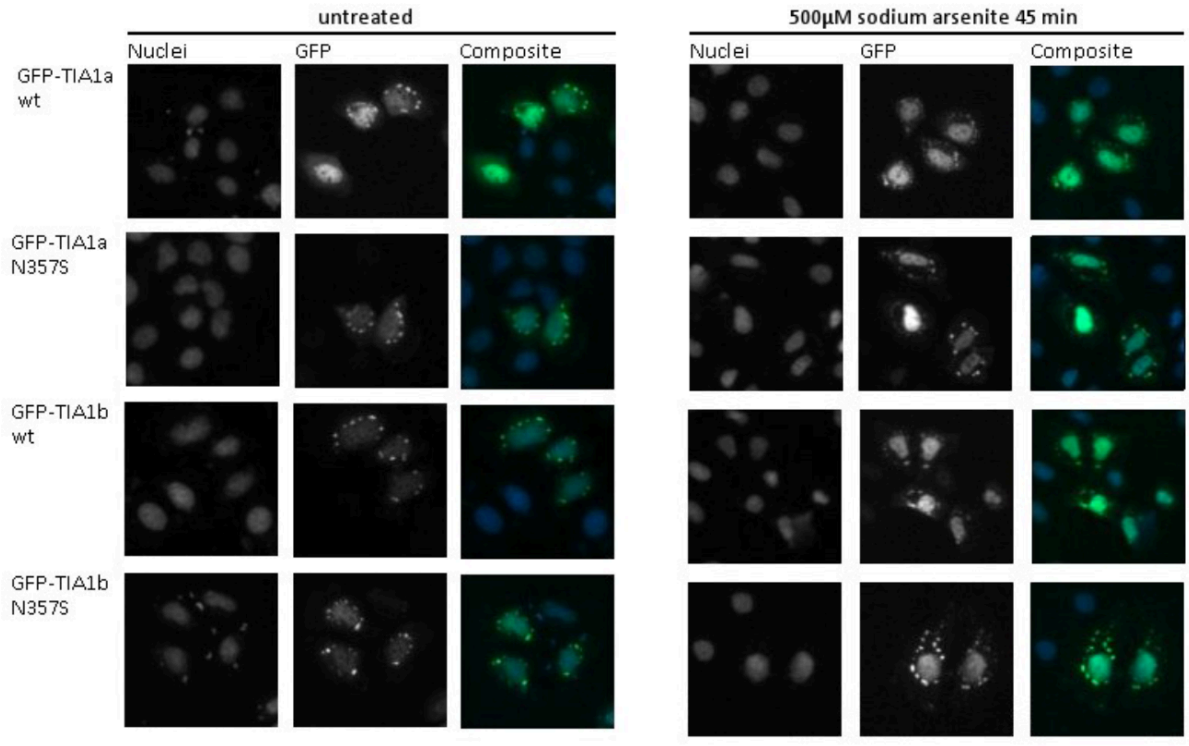

Figure 13. Image of the CellInsight analysis of untreated and sodium arsenite treated GFP-TIA1a and b wt and p.N357S cells. All nuclei are dyed with Hoechst. The GFP-tagged TIA1 is seen localized to the nuclei as well as to the stress granules in the cytosol. Untransfected cells are not seen in the GFP-images, because they do not express the GFP-tagged TIA1 protein.

It has been shown, that the p.E384K change in TIA1 causes a larger amount of stress granules to accumulate in the cytosol as compared to wild-type TIA1 both in untreated and arsenite treated cells (Hackman et al. 2013). It was hence expected, that the p.N357S change would cause a similar change in behavior of the protein.

Unfortunately a portion of the data for the untreated TIA1a p.N357S didn't meet quality standards and had to be excluded. The excluded cases were confirmed by manually investigating the primary imaging data and confirming bad quality of images or signal. Thus, the sample size was reduced, and there was additionally a large variance in the data values. No significant difference could thus be measured between the untreated TIA1a wild-type and p.N357S (shown in **Fig. 14**).

In contrast to the untreated samples, a difference in stress granule number per cell was recorded in the arsenite treated samples. A number of wells had to be omitted from the analysis due to bad quality and lack of signal (confirmed as earlier). The significance of the difference was calculated by the 2-tailed Mann-Whitney U test, which returned a *p* value of 0.05 (shown in **Fig. 14**).

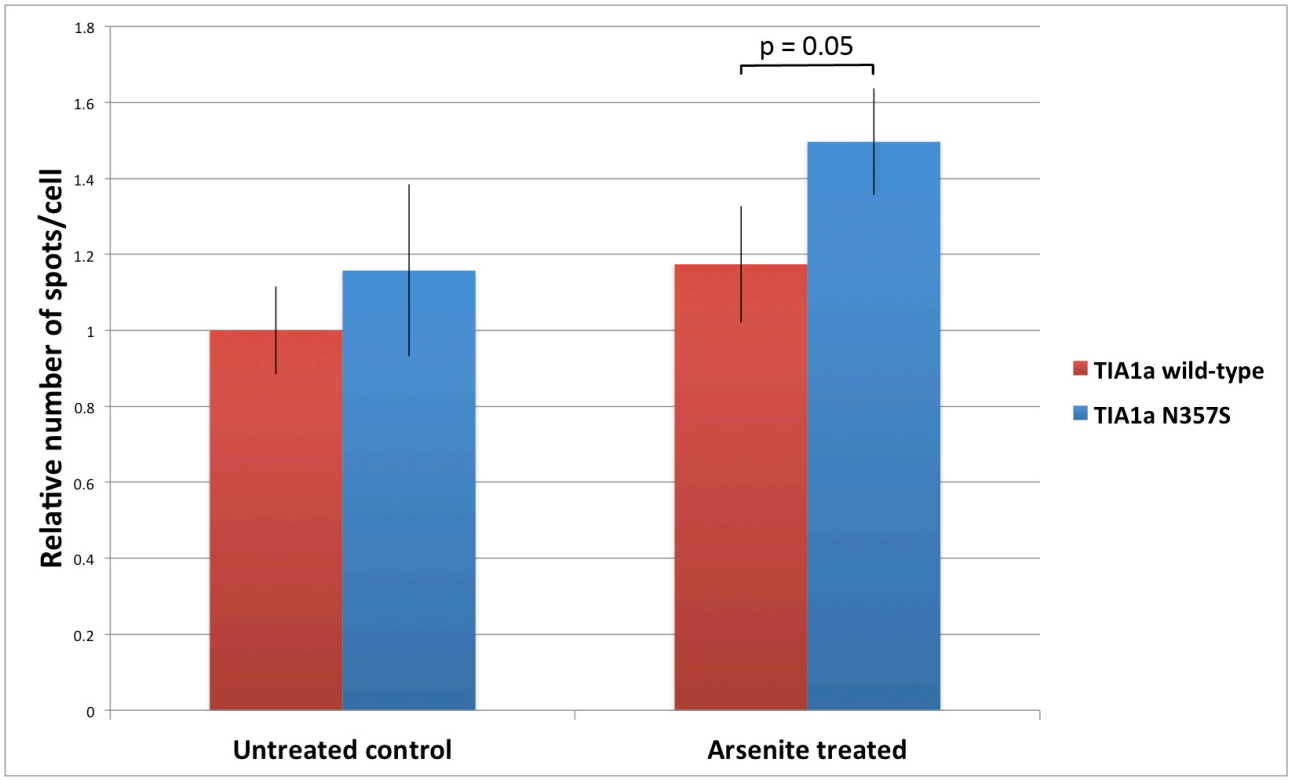

Figure 14. CellInsight spot count data. Each column represents the relative amount of stress granules per analyzed cell as compared to the wild-type untreated cells on the respective plate. The error bars represent the normalized standard deviation of the well averages. Data was assembled from 4 plates, altogether 12 wells for TIA1a wild-type untreated, 6 wells for TIA1a p.N357S untreated, 8 wells for TIA1a wild-type arsenite treated and 7 wells for TIA1a p.N357S arsenite treated. The significance level of the difference of the arsenite treated samples is $p = 0.05$. The significance level was calculated according to the 2-tailed Mann-Whitney *U* test.

No significant difference was recorded in spot area measurements and analyzes, which were performed in the same way as the quantification analysis above. The spot size seems to vary a lot in between the groups, indicating that the mutation might not affect the mean stress granule size.

Unfortunately transfections performed with the b isoform of the TIA1b p.N357S construct were systematically unsuccessful, and no data can be presented for the construct. Issues concerning the construct are discussed in the section **10.2. Subproject I specific errors**.

9.1.3. FLUORESCENCE RECOVERY AFTER PHOTOBLEACHING

The FRAP analysis was performed only using isoform a of TIA1 wild-type, p.E384K and p.N357S transfected HeLa cells, as there has been no recorded difference in performance between the isoforms a and b in either the wild-type or the p.E384K mutant, and no difference in performance had been recorded between the isoforms in the p.N357S either.

It has earlier been shown, that the TIA1a p.E384K recovers significantly slower than the TIA1a wild-type after photobleaching. The aim was to recreate the p.E384K experiment and include p.N357S as well to distinguish possible functional differences between these two. The hypothesis was, that the p.N357S mutation would cause a similar decrease in the ability to recover as the p.E384K, as the mutation is in the same domain and could therefore behave similarly.

It seems though, that the p.N357S mutation actually enables the stress granules to recover faster (shown in **Fig. 15**), possibly indicating that the mutation causes the protein to aggregate more easily than either the wild-type or the p.E384K mutated protein.

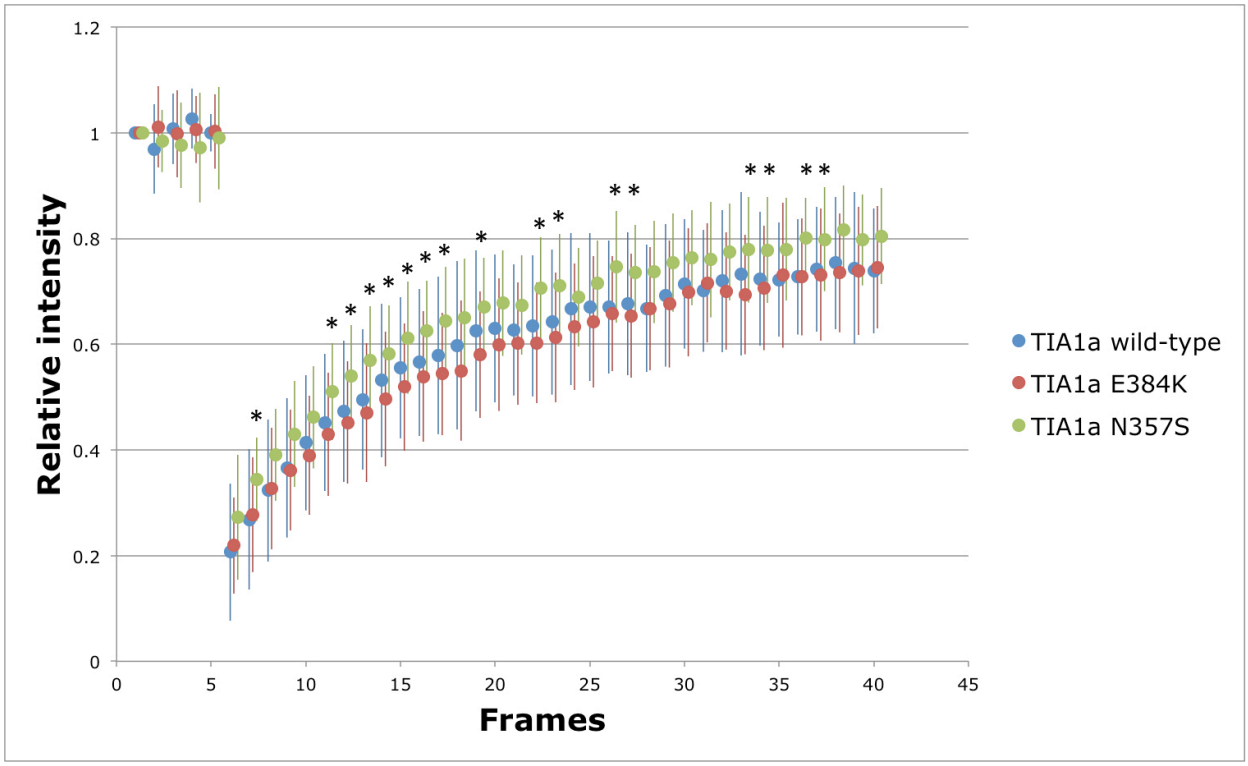

Figure 15. Recovery of relative fluorescence intensity of stress granules after photobleaching in TIA1a wild-type, p.E384K and p.N357S transfected HeLa cells. The values are normalized to the initial intensity of the measured stressgranules. The bleach was induced after frame 5. The frames were taken at 250 ms intervals. The three sample sets are offset by 0.2 arbitrary units on the x-axis to avoid overlap of the representative figures. Significant differences ($p < 0.05$) between TIA1a p.E384K and p.N357S transfected cells are marked with and asterisk (*). *P* value calculated according to the 2-tailed Mann-Whitney *U* test.

Significant levels of difference could not be retrieved for the difference between the recovery of TIA1a wild-type and p.E384K stress granules, which has earlier been done (Hackman *et al*. 2013). Also the difference between TIA1a wild-type and p.N357S stress granules turned out to not be significant.

However, a significant difference in recovery speed between TIA1a p.E384K and p.N357S was recorded. This would indicate, that the p.N357S change causes a different behavior to that of the Welander causing p.E384K change. The question remains whether the p.N357S behaves differently as compared to the wild-type.

Although the results did not return significant values in statistical tests, the trend shown by **figure 15** could indicate, that the p.N357S change actually causes the protein to recover faster than the wild-type. As the change is in fact located in the PRD domain, which brings the protein its aggregation feature, it is plausible that any change in the domain in question would cause the protein to behave differently in aggregative situations.

9.2. SUBPROJECT II: THE EFFECT OF COLD SHOCK ON STRESS GRANULES

The effect of cold shock on stress granules has previously been investigated by Hofmann *et al.* (2012), who concluded that stress granules form at between 4 to 10 h in several different mammalian cell lines, when they are kept at 10°C. The idea was to recreate the experiment using GFP-tagged TIA1 as a stress granule marker to look at whether any significant differences are prevalent between wild-type and p.E384K transfected cells. An untreated and arsenite treated control was included in the experiment.

What could directly be concluded from the results was, that the cells did not react well to the cold shock. Stress granule levels in untreated control cells were significantly higher than in cold shock treated cells (shown in **Fig. 16**). This is due to transfected HeLa cells over-expressing protein, and TIA1's ability to create stress granules when over-expressed.

Cold shock treated cells, on the other hand, go into a hibernation-like state, where their whole machinery is slowed down, the translation of protein and thus the rapid formation of stress granules included. One would think that keeping the cells in colder temperatures for a longer period of time would give them enough time to create stress granules regardless of the temperature, but unfortunately HeLa cells didn't seem to take the cold too well, and longer treatment times were performed at the cost of cell viability.

What is interesting in the results is the observable trend that each series follows the same pattern. Wild-types show smaller amounts of stress granules per cell than their respective p.E384K variants in untreated, arsenite treated and cold shock treated sets. Cold shocked cells showed somewhere between 60 and 75% of stress granules of their untreated controls, and the arsenite treated cells showed systematically more stress granules than either the untreated controls and the cold shock cells.

There was no observed difference between the two isoforms in either the wild-type or the p.E384K samples. No difference has been recorded earlier either.

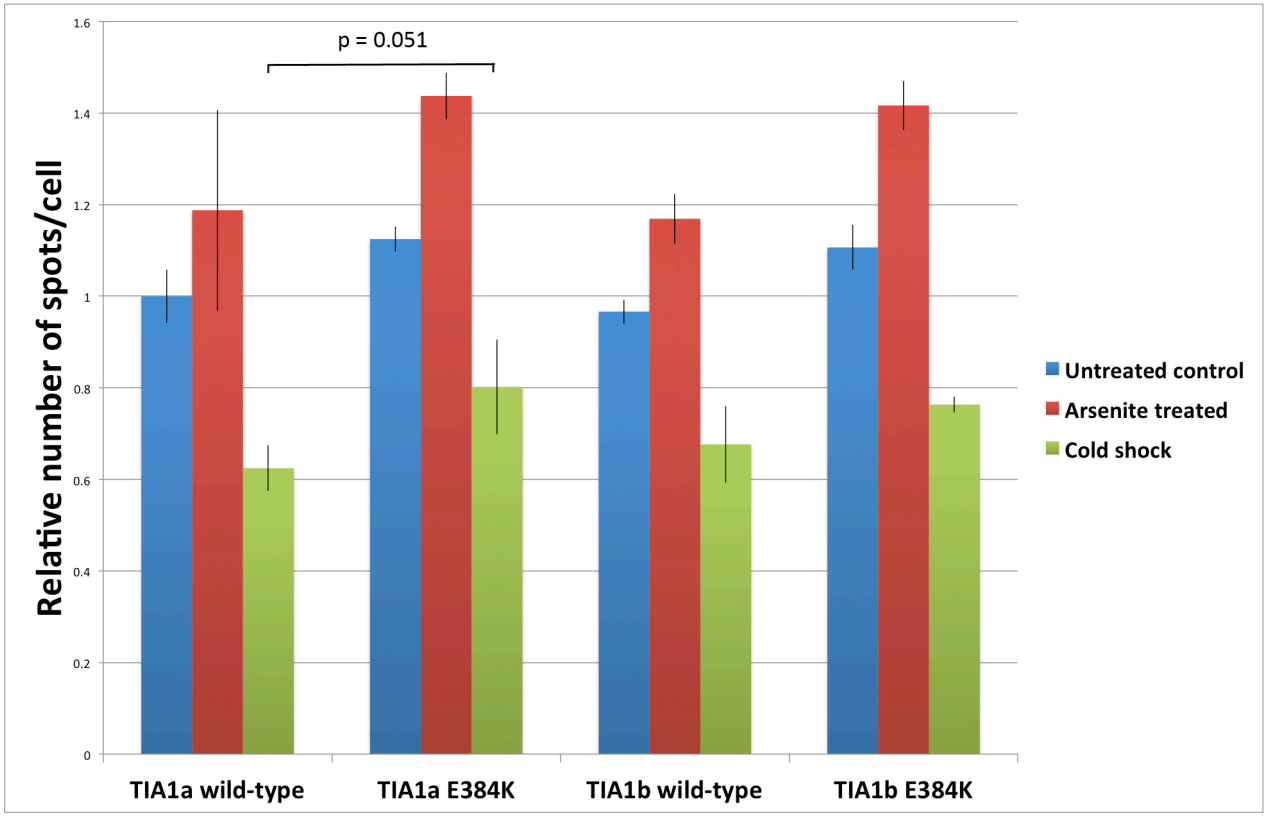

Figure 16. CellInsight spot count data. Each column represents the relative amount of stress granules per analyzed cell as compared to the wild-type untreated cells on the respective plate. The error bars represent the normalized standard deviation of the well averages. Data was assembled from 2 plates, altogether 3 wells for each sample. The significance level (*p* value) of the difference between all untreated, arsenite treated and cold shock treated samples in each group is <0.05, except for the difference between the untreated and arsenite treated TIA1a wild-type. The significance level between the cold shocked TIA1a wild-type and p.E384K was 0.051. The significance level between the cold shocked TIA1b wild-type and p.E384K was 0.108. The significance level was calculated according to an independent sample T-test.

10. EVALUATION OF SOURCES OF ERROR

The variance in data observed between different experiments is partially explained by lack of routine and thus inconsistency in the methods. This could have been corrected by increasing attentiveness in the work and increasing care in general, although everything was performed with the most care possible at the time being. Adopting a consistent routine would also lead to all steps being performed at a higher and more regular pace, leading less differences between different sample sets.

The whole process of creating, imaging and analyzing data for the CellInsight platform is rather long and scattered with possible bottlenecks. The cells have to be transfected, stressed and fixed, imaged and then analyzed. If an error is made at one of these points, the resulting data will be compromised or return null results – for example, if the CellInsight instrument images pictures of low quality due to an unsuccessful transfection or fixation of the cells, the SpotCount software will not be able to return valid data for the well or plate in question.

In addition to problems related to sample treatment, tilts, bends, and scratches of the plate lead to imaging problems. The CellInsight apparatus is unable to focus properly if the plate is somehow damaged. These damages can appear during laboratory work, but also during manufacturing and shipping, and are virtually impossible to observe by the naked eye.

In practice, there was sometimes problems with transfection, which probably were caused by loss of attentiveness during work, pipetting errors and other mundane sources of error, that eventually resulted in loss of (analyzable) data. However, this is probably a minor factor.

Also, when plating cells on a 24-well plate, it should be noted that they easily accumulate on the edges of the well, if plated with too much force or velocity. If the cells are accumulated at the borders of the well, it causes problems at the imaging, as the CellInsight platform's focus capacity is best in the middle of a well and it is thus preferable to image the center, rather than the edges of the well. Therefore, if the cells are attached in the outskirts of the well and the middle is rather scarcely plated, the amount and quality of the acquired data might be reduced.

Part of the data had to be omitted from the analysis due to different reasons (such as the aforementioned issues), causing the results to be based on less data than what would be optimal.

The only way to correct this would be to repeat the experiments, and paying close attention to the now known tricky phases of the protocols. Assuming that the samples have been successfully produced, fixed plates could be imaged again and already existing images could be reanalyzed by running them through the software with an optimized protocol.

10.1. SUBPROJECT I SPECIFIC ERRORS

Transfection issues were more prominent in subproject I than in subproject II. Of the two created constructs, the isoform b did not transfect properly into the cells and data for that isoform was thus lacking. As the error seems to systemically appear for all isoform b p.N357S transfected cells even on the same plates where the isoform a is transfected as expected, it seems more plausible that there is an error in the pEGFP-TIA1b p.N357S plasmid itself, rather than in the methods used.

The plasmid sequence was analyzed and confirmed by sequencing only for the insert and the flanking sequences of the plasmid. There might thus be unnoticed errors in the plasmid sequence. The transfection problems may also be caused by a contamination in the plasmid sample. However, there should be no reason to believe that these would be the primary reasons for the transfection difficulties and problems with the isoform b.

The FRAP analysis was performed within 55 minutes after the arsenite treatment. It is known, that stress granules start to dissolve within minutes of stress relief, but seen that the stress granule number in the transfected cells analyzed did not seem to significantly decrease within this time frame, this does not appear to be an issue in these experiments.

In addition, each analyzed stress granule's frames are taken at slightly different time points due to the instrument's features, resulting in that the same frame number for two different analyzed cells might not be taken at the exact same millisecond after bleaching. The process of normalizing the time points was, however, not performed. In stead it was assumed, that the time difference was negligible, and that the intensity levels for each frame were comparable with one another. This may or may not affect the FRAP results. The sample order was changed between different analysis times, so this should, however, not be an issue.

10.2. SUBPROJECT II SPECIFIC ERRORS

There were several problems faced throughout the cold shock experiment, and it called for a lot of problem solving and application of inventive solutions, unfortunately resulting in rather inconsistent results. The protocol used was based on the Hofmann *et al.* 2012 paper, but there were several differences to the Hofmann experiment, among others the lack of similar premises.

Ideally, the untreated control would be included on the same 24-well-plate as the cold shock treated cells. This could not be executed, as there are no means of thermally insulating the plate in half. The only option would have been to only seed cells in the outermost wells and create thermal insulates for the two halves. This would have significantly reduced the sample size per plate and been difficult to implement in practice. Thus, I opted for accuracy in seeding and handling of the cold shock and control cells and kept them on separate plates.

The cold shock was performed paying attention and recording possible factors affecting the temperature, such as draft. The lead blocks on which the plates were placed were pre-chilled to the ambient temperature, which should be stable enough. However, the effect of draft caused by opening the door of the cold room and warm air flowing in to the room cannot be completely neglected, and could not be controlled either. Ideally, the cold shock would be performed in a completely insulated space with possibility to accurately regulate the temperature, such as a cooling centrifuge or optimally a cooling incubator.

The big variability in the cold shock CellInsight results is a direct cause of the inconsistent experiment conditions. The results were also compromised by the HeLa cells, which did not react well to the treatment, and were thus omitted in the SpotCount analysis by the software due to abnormal cell and nuclei shape. A significant level of cell death due to cold shock was also observed, obviously compromising the results.

The Hofmann paper (Hofmann *et al*. 2012) used significantly longer treatment times for the cells (10 h), but it is also to be noted that their experiment used untransfected COS7 cells and their confirmed hypothesis was that cold-shock induces stress granules formation. The mention of stress granule formation in HeLa cells is very brief and only performed as a control in their article.

It could be considered to do the cold shock in lower temperatures and reducing the exposure time significantly, thus not having to expose the cells to mild cold temperatures during longer times, which they do not seem to take well, as the imaging of the plates revealed an abnormal amount of dead cells. However, if the temperature is lowered too much, the cells risk to slow down their machinery so much, that they would outright stop all their metabolic activity in stead of the treatment inducing a stress response. Another option would be to increase the temperature to somewhere between 37 °C and the used 9-12 °C and significantly increase the treatment time as to see if the treatment would work as intended.

Due to the different behavior of p.N357S and p.E384K in stress granule dynamics, it would be of interest to repeat the cold shock test with a larger set of data with both constructs and considering alternative methods to the conduct of the test. A better way to stabilize the temperature and a more consistent exposure to the cold shock could be considered.

In addition, it could be considered to change cell line for the cold shock experiment. Hofmann *et al.* successfully used COS7 cells in their experiment. Experimenting whether the loss of viability in HeLa cells is caused by the transfection or the cold shock should be established, alongside with whether COS7 tolerate the treatment when transfected and over-expressing as well.

11. CONCLUSIONS AND FUTURE PROSPECTS

The findings of this project do suggest that the p.N357S change in TIA1 has an effect on the protein, changing its functional properties. The results indicate that the mutation may lead to the protein being more prone to aggregate with itself, thus creating stress granules that may assemble faster than the wild type (unconfirmed) and the Welander-causing p.E384K change protein (confirmed).

Since the mutation is located in the PRD domain, which is in charge of the protein's aggregation feature, the belief that the p.N357S change would have an impact on the aggregative attributes of the translated protein are not far fetched.

Within the PRD domain, the Welander causing p.E384K change changes the amino acid residue of glutamic acid to a lysine by a single base pair change. Glutamic acid is a negatively charged amino acid harboring a carboxyl group in its chain, and also acidic, as indicated in its name. Lysine, on the other hand, is positively charged due to its amino group in its chain and has basic features. There is thus a significant difference in the attributes of these two amino acids, which seems to correlate with the functionality of the protein.

In the case of the p.N357S mutation, an asparagine is exchanged for a serine in the amino acid sequence of the protein. Both amino acids belong to the group of amino acids with side chains that are uncharged, yet polar. Serine harbors a hydroxyl group at its free end, while asparagine harbors an amide group.

The experiments with TIA1 harboring the p.N357S change have not been conducted earlier, and it is not known whether similar experiments have been performed elsewhere during this thesis process. The results acquired are thus, as far as known, new to science.

It is not known, whether cold shock experiments with HeLa cells over-expressing any stress granule containing proteins have been conducted earlier or during this thesis process. The results indicate, that the process may be hard and that the cold shock protocol calls for optimization in order to yield trustful results. Although the results were narrow, it was shown that HeLa cells do indeed form stress granules under cold-shock, and a trend for p.E384K cells to accumulate more granules than the wild-type expressing cells was also noticed, although not significant.

Due to the different behavior of p.N357S and p.E384K, it would be of interest to repeat the cold shock test with a larger set of data with both constructs and considering alternative methods to the conduct of the test, along with an optimization of the protocol. A better way to stabilize the temperature and a more consistent exposure to the cold shock should be considered.

As it is known that the p.E384K mutation in TIA1 is responsible for causing Welander Distal Myopathy, the idea of the p.N357S change to be pathogenic is therefore not too far fetched. During the time of this project, other studies done at Folkhälsan Research Center found even more of the p.N357S change in patients with a Welander-like phenotype. However, the mutation appears to occur in connection with other mutations, leading to the belief that it might be involved in a myopathy with a polygenic background (personal communication). Distal myopathies have long been considered diseases of monogenic background, and this finding might revolutionize the field.

Thus, the research will continue and tests are to be made using the p.N357S construct in connection with the other genetic mutations in order to reveal whether these changes are pathogenic.

ACKNOWLEDGEMENTS

This Pro gradu thesis was conducted at Prof. Bjarne Udd's research group at the Folkhälsan Research Center's Institute of Genetics and the University of Helsinki. The work was funded by Samfundet Folkhälsan i svenska Finland rf and Jane and Aatos Erkko foundation.

I wish to thank my supervisors Doc. Peter Hackman, PhD Per-Harald Jonson and FD Jaakko Sarparanta for the guidance and support during the process. I want to thank all the members of the Udd group for welcoming me to the team and taking care of me. I also wish to thank Bjarne Udd for the opportunity to complete this stage of my studies in his group.

I thank the people at the Biomedicum Imaging Unit and the Institute of Biotechnology Light Microscopy Unit at the University of Helsinki for all the help given during the imaging studies.

Furthermore I want to thank all the people at Folkhälsan Reseach Center for contributing to my positive experience. You are wonderful people.

I am grateful for having had Pekka Heino as my coordinator during my studies. He has taught me that there is always a way to make things work out, it's merely a question of finding out how.

An ever so grateful mention goes to my family; Sirkku, Kalle and Arska, for always being there for me. To Erno, who stuck with me through it all. To all my friends for providing unvaluable peer support and much needed getaways from day-to-day life.

Helsinki, August 2015 Lydia Sagath

REFERENCES

Åhlberg, G., Jakobsson, F., Fransson, A., Moritz, A., Borg, K. & Edström, L. 1994, "Distribution of muscle degeneration in Welander distal myopathy - a magnetic resonance imaging and muscle biopsy study", *Neuromuscular disorders,* vol. 4, no. 1, pp. 55-62.

Åhlberg, G., von Tell, D., Borg, K., Edstrom, L. & Anvret, M. 1999, "Genetic linkage of Welander distal myopathy to chromosome 2p13", *Annals of Neurology,* vol. 46, no. 3, pp. 399-404.

Alberts, B., Johnson, A., Lewis, J., Raff, M., Roberts, K. & Walter, P. 2002, "The Cytoskeleton" in *Molecular Biology of the Cell*, 5th edn, Garland Science, .

Anderson, P. & Kedersha, N. 2008, "Stress granules: the Tao of RNA triage", *Trends in biochemical sciences,* vol. 33, no. 3, pp. 141-150.

Anderson, P., Nagler-Anderson, C., O'Brien, C., Levine, H., Watkins, S., Slayter, H.S., Blue, M.L. & Schlossman, S.F. 1990, "A monoclonal antibody reactive with a 15-kDa cytoplasmic granule-associated protein defines a subpopulation of CD8+T lymphocytes", *The Journal of Immunology,* vol. 144, no. 2, pp. 574-582.

Ansved, T. 2001, "Muscle training in muscular dystrophies", *Acta Physiologica Scandinavica,* vol. 171, no. 3, pp. 359-366.

Antar, L.N., Dictenberg, J.B., Plociniak, M., Afroz, R. & Bassell, G.J. 2005, "Localization of FMRP-associated mRNA granules and requirement of microtubules for activity-dependent trafficking in hippocampal neurons", *Genes, Brain and Behavior,* vol. 4, no. 6, pp. 350-359.

Arimoto, K., Fukuda, H., Imajoh-Ohmi, S., Saito, H. & Takekawa, M. 2008, "Formation of stress granules inhibits apoptosis by suppressing stress-responsive MAPK pathways", *Nature Cell Biology,* vol. 10, no. 11, pp. 1324-1332.

Bolduc, V., Marlow, G., Boycott, K.M., Saleki, K., Inoue, H., Kroon, J., Itakura, M., Robitaille, Y., Parent, L., Baas, F., Mizuta, K., Kamata, N., Richard, I., Linssen, W.H.J.P., Mahjneh, I., de Visser, M., Bashir, R. & Brais, B. 2010, "Recessive Mutations in the Putative Calcium-Activated Chloride Channel Anoctamin 5 Cause Proximal LGMD2L and Distal MMD3 Muscular Dystrophies", *American Journal of Human Genetics,* vol. 86, no. 2, pp. 213-221.

Borg, K., Åhlberg, G., Borg, J. & Edström, L. 1991, "Welander's distal myopathy: clinical, neurophysiological and muscle biopsy observations in young and middle aged adults with early symptoms", *Journal of Neurology, Neurosurgery & Psychiatry,* vol. 54, no. 6, pp. 494-498.

Borg, K., Borg, J. & Lindblom, U. 1987, "Sensory involvement in distal myopathy (Welander)", *Journal of the neurological sciences,* vol. 80, no. 2–3, pp. 323-332.

Buchan, J. ., Kolaitis, R., Taylor, J. . & Parker, R. 2013, "Eukaryotic Stress Granules Are Cleared by Autophagy and Cdc48/VCP Function", *Cell,* vol. 153, no. 7, pp. 1461-1474.

Campbell, N.A., Reece, J.B., Urry, L.A., Cain, M.L., Wasserman, S.A., Minorsky, P.V. & Jackson, R.B. (eds) 2008, *Biology*, 8th edn, Pearson Education.

Cirak, S., Von Deimling, F., Sachdev, S., Errington, W.J., Herrmann, R., Bönnemann, C., Brockmann, K., Hinderlich, S., Lindner, T.H., Steinbrecher, A., Hoffmann, K., Privé, G.G., Hannink, M., Nürnberg, P. & Voit, T. 2010, "Kelch-like homologue 9 mutation is associated with an early onset autosomal dominant distal myopathy", *Brain,* vol. 133, no. 7, pp. 2123-2135.

Craig, R. & Padron, R. 2004, "Myology, Chapter 7: Molecular Structure of the Sarcomere" in *Myology* McGraw-Hill Companies, .

Duff, R.M., Tay, V., Hackman, P., Ravenscroft, G., McLean, C., Kennedy, P., Steinbach, A., Schöffler, W., Van Der Ven, P.F.M., Fürst, D.O., Song, J., Djinovic-Carugo, K., Penttilä, S., Raheem, O., Reardon, K., Malandrini, A., Gambelli, S., Villanova, M., Nowak, K.J., Williams, D.R., Landers, J.E., Brown Jr., R.H., Udd, B. & Laing, N.G. 2011, "Mutations in the N-terminal actin-binding domain of filamin C cause a distal myopathy", *American Journal of Human Genetics,* vol. 88, no. 6, pp. 729-740.

Durmus, H., Laval, S.H., Deymeer, F., Parman, Y., Kiyan, E., Gokyigiti, M., Ertekin, C., Ercan, I., Solakoglu, S., Karcagi, V., Straub, V., Bushby, K., Lochmüller, H. & Serdaroglu-Oflazer, P. 2011, "Oculopharyngodistal myopathy is a distinct entity: Clinical and genetic features of 47 patients", *Neurology,* vol. 76, no. 3, pp. 227-235.

Durmus, H., Laval, S.H., Deymeer, F., Parman, Y., Kiyan, E., Gokyigiti, M., Ertekin, C., Ercan, I., Solakoglu, S., Karcagi, V., Straub, V., Bushby, K., Lochmüller, H. & Serdaroglu-Oflazer, P. 2011, "Oculopharyngodistal myopathy is a distinct entity: Clinical and genetic features of 47 patients", *Neurology,* vol. 76, no. 3, pp. 227-235.

Emery, A.E.H. 2002, "The muscular dystrophies", *The Lancet,* vol. 359, no. 9307, pp. 687-695.

Felice, K.J., Meredith, C., Binz, N., Butler, A., Jacob, R., Akkari, P., Hallmayer, J. & Laing, N. 1999, "Autosomal dominant distal myopathy not linked to the known distal myopathy loci", *Neuromuscular Disorders,* vol. 9, no. 2, pp. 59-65.

Fukuhara, N., Kumamoto, T. & Tsubaki, T. 1980, "Rimmed Vacuoles", *Acta Neuropathologica,* vol. 51, no. 3, pp. 229-235.

Gilks, N., Kedersha, N., Ayodele, M., Shen, L., Stoecklin, G., Dember, L.M. & Anderson, P. 2004, "Stress Granule Assembly Is Mediated by Prion-like Aggregation of TIA-1", *Molecular Biology of the Cell,* vol. 15, no. 12, pp. 5383-5898.

Gowers, W.R. 1902, "A Lecture on Myopathy and a Distal Form", *The British Medical Journal,* vol. 2, no. 2167, pp. 89-92.

Griggs, R. & Markesby, W. 1994, "Distal myopathies" in *Distal Myopathies*, ed. F.C. Engel A., McGraw-Hill Companies, , pp. 1246-1257.

Griggs, R., Vihola, A., Hackman, P., Talvinen, K., Haravuori, H., Faulkner, G., Eymard, B., Richard, I., Selcen, D., Engel, A., Carpen, O. & Udd, B. 2007, "Zaspopathy in a large classic late-onset distal myopathy family", *Brain,* vol. 130, no. 6, pp. 1477-1484.

Hackman, P., Sarparanta, J., Lehtinen, S., Vihola, A., Evila, A., Jonson, P.H., Luque, H., Kere, J., Screen, M., Chinnery, P.F., Åhlberg, G., Edstrom, L. & Udd, B. 2013, "Welander distal myopathy is caused by a mutation in the RNA-binding protein TIA1", *Annals of Neurology,* vol. 73, no. 4, pp. 500-509.

Harding, H.P., Novoa, I., Zhang, Y., Zeng, H., Wek, R., Schapira, M. & Ron, D. 2000, "Regulated translation initiation controls stress-induced gene expression on mammalian cells", *Molecular Cell,* vol. 6, no. 5, pp. 1099-1108.

Harding, H.P., Zhang, Y., Bertolotti, A., Zeng, H. & Ron, D. 2000, "Perk is essential for translational regulation and cell survival during the unfolded protein response", *Molecular Cell,* vol. 5, no. 5, pp. 897-904.

Hofmann, S., Cherkasova, V., Bankhead, P., Bukau, B. & Stoecklin, G. 2012, "Translation suppression promotes stress granule formation and cell survival in response to cold shock", *Molecular biology of the cell,* vol. 23, no. 19, pp. 3786-3800.

Holcik, M. & Sonenberg, N. 2005, "Translational control in stress and apoptosis", *Nature reviews.Molecular cell biology,* vol. 6, no. 4, pp. 318-327.

Illa, I. 2000, "Distal Myopathies", *Journal of Neurology,* vol. 247, no. 3, pp. 169-174.

Ivanov, P.A., Chudinova, E.M. & Nadezhdina, E.S. 2003, "Disruption of microtubules inhibits cytoplasmic ribonucleoprotein stress granule formation", *Experimental Cell Research,* vol. 290, no. 2, pp. 227-233.

Kawai, T., Fan, J., Mazan-Mamczarz, K. & Gorospe, M. 2004, "Global mRNA stabilization preferentially linked to translational repression during the endomplasmic reticulum stress response", *Molecular Cell Biology,* vol. 24, pp. 6773-6787.

Kawakami, A., Tian, Q., Duan, X., Streuli, M., Schlossman, S.F. & Anderson, P. 1992, "Identification and functional characterization of a TIA-1-related nucleolysin", *Proceedings of the National Academy of Sciences of the United States of America,* vol. 89, no. 18, pp. 8681-8685.

Kedersha, N. & Anderson, P. 2002, "Stress granules: sites of mRNA triage that regulate mRNA stability and translatability", *Biochemical Society transactions,* vol. 30, no. Pt 6, pp. 963-969.

Kedersha, N., Chen, S., Gilks, N., Li, W., Miller, I.J., Stahl, J. & Anderson, P. 2002, "Evidence that ternary complex (eIF2-GTP-tRNA(i)(Met))-deficient preinitiation complexes are core constituents of mammalian stress granules", *Molecular Biology of the Cell,* vol. 13, no. 1, pp. 195-210.

Kedersha, N., Cho, M.R., Li, W., Yacono, P.W., Chen, S., Gilks, N., Golan, D.E. & Anderson, P. 2000, "Dynamic shuttling of TIA1 accompanies the recruitment of mRNA to mammalian stress granules", *Journal of Cell Biology,* vol. 151, no. 6, pp. 1257-1268.

Kedersha, N., Gupta, M., Li, W., Miller, I. & Anderson, P. 1999, "RNA-binding proteins TIA-1 and TIAR link the phosphorylation of eIF-2 alpha to the assembly of mammalian stress granules", *Journal of Cell Biology,* vol. 147, no. 7, pp. 1431-1442.

Kedersha, N., Stoecklin, G., Ayodele, M., Yacono, P., Lykke-Andersen, J., Fritzler, M.J., Scheuner, D., Kaufman, R.J., Golan, D.E. & Anderson, P. 2005, "Stress granules and processing bodies are dynamically linked sites of mRNP remodeling", *Journal of Cell Biology,* vol. 169, no. 6, pp. 871-884.

Kim, W.J., Back, S.H., Kim, V., Ryu, I. & Jang, S.K. 2005, "Sequestration of TRAF2 into stress granules interrupts tumor necrosis factor signaling under stress conditions", *Molecular Cell Biology,* vol. 25, no. 6, pp. 2450-2462.

Klar, J., Sobol, M., Melberg, A., Mabert, K., Ameur, A., Johansson, A.C., Feuk, L., Entesarian, M., Orlen, H., Casar-Borota, O. & Dahl, N. 2013, "Welander distal myopathy caused by an ancient founder mutation in TIA1 associated with perturbed splicing", *Human mutation,* vol. 34, no. 4, pp. 572-577.

Laing, N.G., Laing, B.A., Meredith, C., Wilton, S.D., Robbins, P., Honeyman, K., Dorosz, S., Kozman, H., Mastaglia, F.L. & Kakulas, B.A. 1995, "Autosomal dominant distal myopathy: Linkage to chromosome 14", *American Journal of Human Genetics,* vol. 56, no. 2, pp. 422-427.

Linssen, W.H.J.P., De Visser, M., Notermans, N.C., Vreyling, J.P., Van Doorn, P.A., Wokke, J.H.J., Baas, F. & Bolhuis, P.A. 1998, "Genetic heterogeneity in miyoshi-type distal muscular dystrophy", *Neuromuscular Disorders,* vol. 8, no. 5, pp. 317-320.

MacIntosh, P., Gardiner, P. & McComas, A. 2006, *Skeletal Muscle - Form and Function,* 2nd edn, Human Kinetics.

Mahjneh, I., Haravuori, H., Paetau, A., Anderson, L.V.B., Saarinen, A., Udd, B. & Somer, H. 2003, "A distinct phenotype of distal myopathy in a large Finnish family", *Neurology,* vol. 61, no. 1, pp. 87-92.

Malicdan, M.C. & Nonaka, I. 2008, "Distal myopathies a review: highlights on distal myopathies with rimmed vacuoles", *Neurology India,* vol. 56, no. 3, pp. 314-324.

Marieb, E.N. & Hoehn, K. 2009, *Human Anatomy & Physiology,* 7th edn, Pearson Education.

Mastaglia, F.L. 1999, "Distal myopathies: clinical and molecular diagnosis and classification", *Journal of Neurology, Neurosurgery & Psychiatry,* vol. 67, pp. 703-707.

McEwen, E., Kedersha, N., Song, B., Schenuer, D., Gilks, N., Han, A., Chen, J.J., Anderson, P. & Kaufman, R.J. 2005, "Heme-regulated inhibitor kinase-mediated phosphorylation of eukaryotic translation initiation factor 2 inhibits translation, induces stress granule formation, and mediates survival upon arsenite exposure", *Journal of Biological Chemistry,* vol. 208, no. 17, pp. 16925-16933.

Miyoshi, K., Kawai, H., Iwasa, M., Kusaka, K., Nishino, H. 1986, "Autosomal recessive distal muscular dystrophy as a new type of progressive muscular dystrophy; seventeen cases in eight families including and autopsied case", *Brain*, vol. 109, pp. 31-54.

Moeller, B.J., Cao, Y. & Dewhirst, M.W. 2004, "Radiation activates HIF-1 to regulate vascular radiosensitivity in tumors: role of reoxigenation, free radicals, and stress granules.", *Cancer Cell,* vol. 5, no. 5, pp. 429-441.

Nonaka, I., Sunohara, N., Ishiura, S. & Satoyoshi, E. 1981, "Familial distal myopathy with rimmed vacuole and lamellar (myeloid) body formation", *Journal of the neurological sciences,* vol. 51, no. 1, pp. 141-155.

Palmio, J., Sandell, S., Suominen, T., Penttilä, S., Raheem, O., Hackman, P., Huovinen, S., Haapasalo, H. & Udd, B. 2011, "Distinct distal myopathy phenotype caused by VCP gene mutation in a Finnish family", *Neuromuscular Disorders,* vol. 21, no. 8, pp. 551-555.

Pénisson-Besnier, I., Talvinen, K., Dumez, C., Vihola, A., Dubas, F., Fardeau, M., Hackman, P., Carpen, O. & Udd, B. 2006, "Myotilinopathy in a family with late onset myopathy", *Neuromuscular disorders,* vol. 6, pp. 427-431.

Reilich, P., Schoser, B., Schramm, N., Krause, S., Schessl, J., Kress, W., Müller-Höcker, J., Walter, M.C. & Lochmuller, H. 2010, "The p.G154S mutation of the alpha-B crystallin gene (CRYAB) causes late-onset distal myopathy", *Neuromuscular Disorders,* vol. 20, no. 4, pp. 255-259.

Senderek, J., Garvey, S.M., Krieger, M., Guergueltcheva, V., Urtizberea, A., Roos, A., Elbracht, M., Stendel, C., Tournev, I., Mihailova, V., Feit, H., Tramonte, J., Hedera, P., Crooks, K., Bergmann, C., Rudnik-Schöneborn, S., Zerres, K., Lochmüller, H., Seboun, E., Weis, J., Beckmann, J.S., Hauser, M.A. & Jackson, C.E. 2009, "Autosomal-Dominant Distal Myopathy Associated with a Recurrent Missense Mutation in the Gene Encoding the Nuclear Matrix Protein, Matrin 3", *American Journal of Human Genetics,* vol. 84, no. 4, pp. 511-518.

Servidei, S., Capon, F., Spinazzola, A., Mirabella, M., Semprini, S., De Rosa, G., Gennarelli, M., Sangiuolo, F., Ricci, E., Mohrenweiser, H.W., Dallapiccola, B., Tonali, P. & Novelli, G. 1999, "A distinctive autosomal dominant vacuolar neuromyopathy linked to 19p13", *Neurology,* vol. 53, no. 4, pp. 830-837.

Silverthorn, D.U. 2010, "Muscles" in *Human Physiology: An Integrated Approach*, ed. D. Espinoza, 5th edn, Pearson Benjamin Cummings, , pp. 406-466.

Sjöberg, G., Saavedra-Matiz, C.A., Rosen, D.R., Wijsman, E.M., Borg, K., Horowitz, S.H. & Sejersen, T. 1999, "A missense mutation in the desmin rod domain is associated with autosomal dominant distal myopathy, and exerts a dominant negative effect on filament formation", *Human molecular genetics,* vol. 8, no. 12, pp. 2191-2198.

Srivastava, S.P., Kumar, K.U. & Kaufman, R.J. 1998, "Phosphorylation of Eukaryotic Translation Initiation Factor 2 Mediates Apoptosis in Response to Activation of the Double-stranded RNA-dependent Protein Kinase", *Jounral of Biological Chemistry,* vol. 273, no. 4, pp. 2416-2423.

Stone, R. & Stone, J. 2006, *Atlas of skeletal muscles,* McGraw-Hill Companies.

Tian, Q., Streuli, M., Saito, H., Schlossman, S.F. & Anderson, P. 1991, "A polyadenylate binding protein localized to the granules of cytolytic lymphocytes induces DNA fragmentation in target cells", *Cell,* vol. 67, no. 3, pp. 629-639.

Udd, B. 2012, "Distal myopathies - New genetic entities expand diagnostic challenge", *Neuromuscular disorders,* vol. 22, no. 1, pp. 5-12.

Udd, B. 2014, "Chapter 27: Distal and myofibrillar myopathies" in *Oxford Textbook of Neuromuscular Disorders*, eds. D. Hilton-Jones & M.R. Turner, Oxford University Press, , pp. 264-276.

Udd, B., Partanen, J., Halonen, P., Falck, B., Hakamies, L., Heikkila, H., Ingo, S., Kalimo, H., Kaariainen, H., Laulumaa, V., Paljarvi, L., Rapola, J., Reunanen, M., Sonninen, V. & Somer, H. 1993, "Tibial muscular dystrophy: Late adult-onset distal myopathy in 66 Finnish patients", *Archives of Neurology,* vol. 50, no. 6, pp. 604-608.

Wallgren-Pettersson, C., Lehtokari, V.-., Kalimo, H., Paetau, A., Nuutinen, E., Hackman, P., Sewry, C., Pelin, K. & Udd, B. 2007, "Distal myopathy caused by homozygous missense mutations in the nebulin gene", *Brain,* vol. 130, no. 6, pp. 1465-1476.

Wang, I., Hennig, J., Jagtap, P.K.A., Sonntag, M., Valcárel, J. & Sattler, M. 2014, "Structure, dynamics and RNA binding of the multi-domain splicing factor TIA1", *Nucleic Acids Research,* vol. 42, no. 9, pp. 5949-5966.

Wek, S.A., Zhu, S. & Wek, R.C. 1995, "The histidyl-tRNA synthetase-related sequence in the eIF-2 alpha protein kinase GCN2 interacts with tRNA and is required for activation in response to starvation for different amino acid", *Molecular Cell Biology,* vol. 15, no. 8, pp. 4497-4506.

Welander, L. 1951, "Myopathia distalis tarda hereditaria", *Acta Medica Scandinavica,* vol. 141, pp. 1-142.

Welander, L. 1957, "Homozygous appearance of distal myopathy", *Acta Genetica et Statistica Medica,* vol. 7, no. 2, pp. 321-325.

Zhang, T., Delestienne, N., Huez, G., Kruys, V. & Gueydan, C. 2005, "Identification of the sequence determinants mediating the nucleo-cytoplasmic shuttling of TIAR and TIA-1 RNA-binding proteins", *Jorunal of Cell Science,* vol. 118, no. 23, pp. 5453-5463.

SUPPLEMENTS

SUPPLEMENT 1: The pEGFP plasmid map

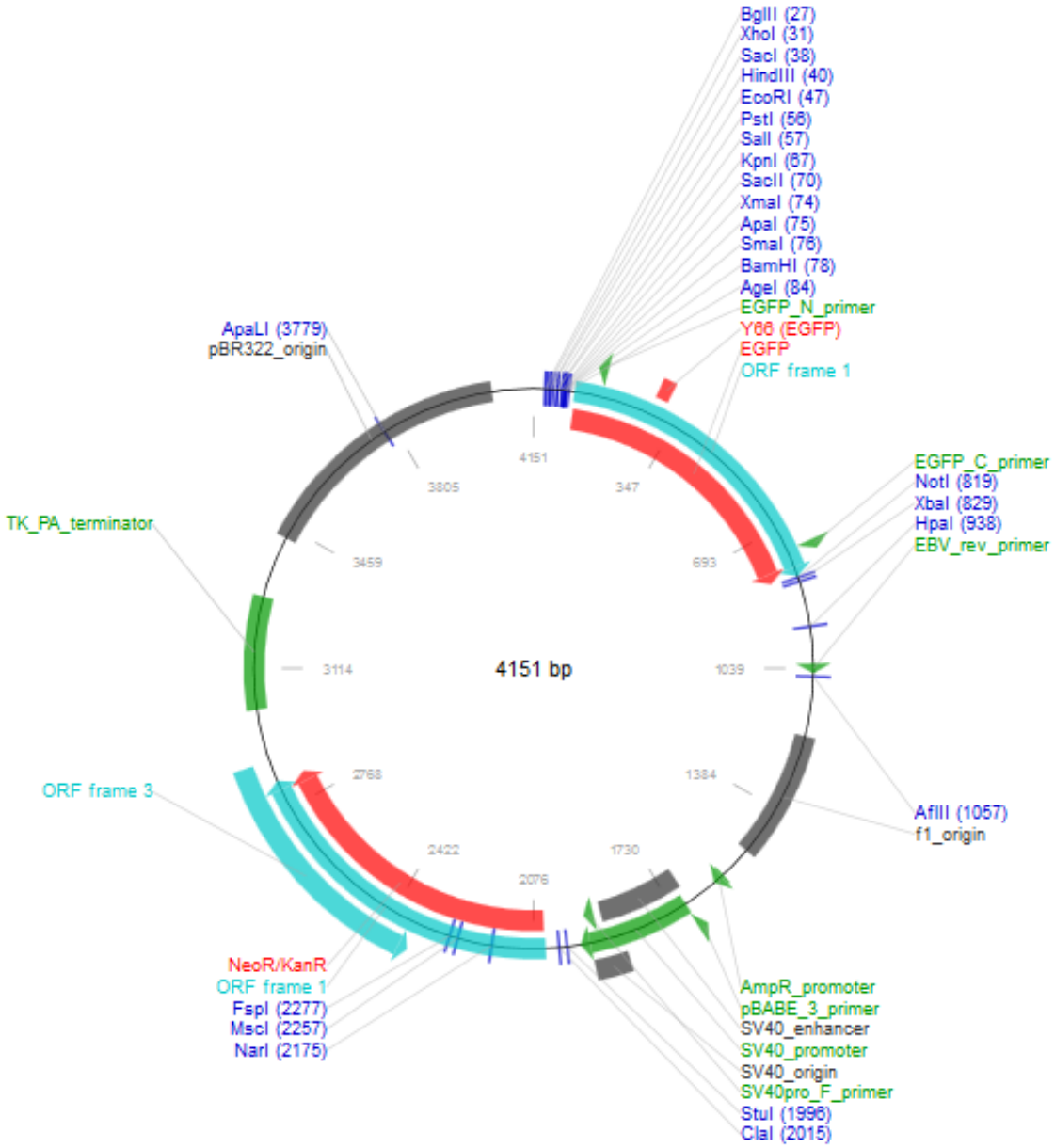

The TIA1a insert is located between the BamHI and HindIII sites in the multiple cloning site of the pEGFP plasmid. Plasmid map from AddGene (https://www.addgene.org/vector-database/2491/).

SUPPLEMENT 2: Mutagenic PCR conditions

Forward primer: `5'-[phos]CACCATGGATGGGACCAA-3'`
Reverse primer: `5'-[phos]AGGCGGTTGCACTCCATAAC-3'`

Tm calculator:
https://www.lifetechnologies.com/fi/en/home/brands/thermo-scientific/molecular-biology/molecular-biology-learning-center/molecular-biology-resource-library/thermo-scientific-web-tools/tm-calculator.html

Table A. Mutagenic PCR reaction mix for pEGFP-TIA1 p.N357S point mutation induction using Phusion polymerase.

Reagent	Amount/reaction	Specification
Water	12.4 µl	MilliQ
Phusion buffer (5x)	4.0 µl	Phusion High-Fidelity buffer
10 mM dNTPs	0.4 µl	dATP, dCTP, dGTP, dTTP, 2.5 mM each
10 µM forward primer	1.0 µl	
10 µM reverse primer	1.0 µl	
Template DNA (10 ng/µl)	1.0 µl	
Enzyme	0.2 µl	Phusion High-Fidelity DNA Polymerase
Σ	20 µl	

Table B. Mutagenic PCR program for pEGFP-TIA1 p.N357S point mutation induction using Phusion polymerase.

	Phase	Temperature	Time
1	Initial denaturation	98ºC	30 s
2	Denaturation	98ºC	10 s
3	Melting	66ºC	30 s
4	Annealing	72ºC	180 s
5	Final extension	72ºC	10 min
6	Hold	6ºC	Hold
Steps 2-4 repeated 30 times, total time approximately 2 h 15 min.			

SUPPLEMENT 3: TIA1a and b, wt, p.E384K and p.N357S amino acid sequence

Legend:
Amino acid sequence
11 aa sequence unique to isoform a, excluded in b
Isoform dependent variation [a/b]
p.N357S variation [wild-type/mutant]
p.E384K variation [wild-type/mutant]

MEDEMPKTLYVGNLSRDVTEALILQLFSQIGPCKNCKMIMDTAGNDPYCFVEFHEHRHAAAALAAM
NGRKIMGKEVKVNWATTPSSQKKDTSSSTVVSTQRSQ[D/N]HFHVFVGDLSPEITTEDIKAAFAP
FGRISDARVVKDMATGKSKGYGFVSFFNKWDAENAIQQMGGQWLGGRQIRTNWATRKPPAPKSTYE
SNTKQLSYDEVVNQSSPSNCTVYCGGVTSGLTEQLMRQTFSPFGQIMEIRVFPDKGYSFVRFNSHE
SAAHAIVSVNGTTIEGHVVKCYWGKETLDMINPVQQQNQIGYPQPYGQWGQWYGNAQQIGQYMPNG
WQVPAYGMYGQAWNQQGFNQTQSSAPWMGP[N/S]YGVQPPQGQNGSMLPNQPSGYRVAGY[E/K]
TQ

SUPPLEMENT 4: pEGFP-TIA1a and b, wt, p.E384K and p.N357S DNA sequence

Legend:
EGFP plasmid sequence
TIA1 sequence
33 bp sequence unique to isoform a, excluded in b
p.N357S variation [wild-type/mutant]
p.E384K variation |wild-type/mutant]

TAGTTATTAATAGTAATCAATTACGGGGTCATTAGTTCATAGCCCATATATGGAGTTCCGCGTTACATAACTTACGGTAAATGGCCCGCCTGGCTGACCG
CCCAACGACCCCCGCCCATTGACGTCAATAATGACGTATGTTCCCATAGTAACGCCAATAGGGACTTTCCATTGACGTCAATGGGTGGAGTATTTACGGT
AAACTGCCCACTTGGCAGTACATCAAGTGTATCATATGCCAAGTACGCCCCCTATTGACGTCAATGACGGTAAATGGCCCGCCTGGCATTATGCCCAGTA
CATGACCTTATGGGACTTTCCTACTTGGCAGTACATCTACGTATTAGTCATCGCTATTACCATGGTGATGCGGTTTTGGCAGTACATCAATGGGCGTGGA
TAGCGGTTTGACTCACGGGGATTTCCAAGTCTCCACCCCATTGACGTCAATGGGAGTTTGTTTTGGCACCAAAATCAACGGGACTTTCCAAAATGTCGTA
ACAACTCCGCCCCATTGACGCAAATGGGCGGTAGGCGTGTACGGTGGGAGGTCTATATAAGCAGAGCTGGTTTAGTGAACCGTCAGATCCGCTAGCGCTA
CCGGTCGCCACCATGGTGAGCAAGGGCGAGGAGCTGTTCACCGGGGTGGTGCCCATCCTGGTCGAGCTGGACGGCGACGTAAACGGCCACAAGTTCAGCG
TGTCCGGCGAGGGCGAGGGCGATGCCACCTACGGCAAGCTGACCCTGAAGTTCATCTGCACCACCGGCAAGCTGCCCGTGCCCTGGCCCACCCTCGTGAC
CACCCTGACCTACGGCGTGCAGTGCTTCAGCCGCTACCCCGACCACATGAAGCAGCACGACTTCTTCAAGTCCGCCATGCCCGAAGGCTACGTCCAGGAG
CGCACCATCTTCTTCAAGGACGACGGCAACTACAAGACCCGCGCCGAGGTGAAGTTCGAGGGCGACACCCTGGTGAACCGCATCGAGCTGAAGGGCATCG
ACTTCAAGGAGGACGGCAACATCCTGGGGCACAAGCTGGAGTACAACTACAACAGCCACAACGTCTATATCATGGCCGACAAGCAGAAGAACGGCATCAA
GGTGAACTTCAAGATCCGCCACAACATCGAGGACGGCAGCGTGCAGCTCGCCGACCACTACCAGCAGAACACCCCCATCGGCGACGGCCCCGTGCTGCTG
CCCGACAACCACTACCTGAGCACCCAGTCCGCCCTGAGCAAAGACCCCAACGAGAAGCGCGATCACATGGTCCTGCTGGAGTTCGTGACCGCCGCCGGGA
TCACTCTCGGCATGGACGAGCTGTACAAGTCCGGACTCAGATCTCGAGCTCAAGCTTCGAATTCTGCAGTCGACGAGGACGAGATGCCCAAGACTCTATA
CGTCGGTAACCTTTCCAGAGATGTGACAGAAGCTCTAATTCTGCAACTCTTTAGCCAGATTGGACCTTGTAAAAACTGCAAAATGATTATGGATACAGCT
GGAAATGATCCCTATTGTTTTGTGGAGTTTCATGAGCATCGTCATGCAGCTGCAGCATTAGCTGCTATGAATGGACGGAAGATAATGGGTAAGGAAGTCA
AAGTGAATTGGGCAACAACCCCTAGCAGTCAAAAGAAAGATACAAGCAGTAGTACCGTTGTCAGCACACAGCGTTCACAAGATCATTTCCATGTCTTTGT
TGGTGATCTCAGCCCAGAAATTACAACTGAAGATATAAAAGCTGCTTTTGCACCATTTGGAAGAATATCAGATGCCCGAGTGGTAAAAGACATGGCAACA
GGAAAGTCTAAGGGATATGGCTTTGTCTCCTTTTTCAACAAATGGGATGCTGAAAACGCCATTCAACAGATGGGTGGCCAGTGGCTTGGTGGAAGACAAA
TCAGAACTAACTGGGCAACCCGAAAGCCTCCCGCTCCAAAGAGTACATATGAGTCAAATACCAAACAGCTATCATATGATGAGGTTGTAAATCAGTCTAG
TCCAAGCAACTGTACTGTATACTGTGGAGGTGTTACTTCTGGGCTAACAGAACAACTAATGCGTCAGACTTTTTCACCATTTGGACAAATAATGGAAATT
CGAGTCTTTCCAGATAAAGGATATTCATTTGTTCGGTTCAATTCCCATGAAAGTGCAGCACATGCAATTGTTTCTGTTAATGGTACTACCATTGAAGGTC
ATGTTGTGAAATGCTATTGGGGCAAAGAAACTCTTGATATGATAAATCCCGTGCAACAGCAGAATCAAATTGGATATCCCCAACCTTATGGCCAGTGGGG
CCAGTGGTATGGAAATGCACAACAAATTGGCCAGTATATGCCTAATGGTTGGCAAGTTCCTGCATATGGAATGTATGGCCAGGCATGGAACCAGCAAGGA
TTTAATCAGACACAGTCTTCTGCACCATGGATGGGACCAA[A/G]TTATGGAGTGCAACCGCCTCAAGGGCAAAATGGCAGCATGTTGCCCAATCAGCCT
TCTGGGTATCGAGTGGCAGGGTAT[G/A]AAACCCAGTGAAAGGGCGAATTCCAGCACACTGGCGGCCGTTACTAGTGGATCCAAACGGATCTAGATAAC
TGATCATAATCAGCCATACCACATTTGTAGAGGTTTTACTTGCTTTAAAAAACCTCCCACACCTCCCCCTGAACCTGAAACATAAAATGAATGCAATTGT
TGTTGTTAACTTGTTTATTGCAGCTTATAATGGTTACAAATAAAGCAATAGCATCACAAATTTCACAAATAAAGCATTTTTTTCACTGCATTCTAGTTGT
GGTTTGTCCAAACTCATCAATGTATCTTAACGCGTAAATTGTAAGCGTTAATATTTTGTTAAAATTCGCGTTAAATTTTTGTTAAATCAGCTCATTTTTT
AACCAATAGGCCGAAATCGGCAAAATCCCTTATAAATCAAAAGAATAGACCGAGATAGGGTTGAGTGTTGTTCCAGTTTGGAACAAGAGTCCACTATTAA
AGAACGTGGACTCCAACGTCAAAGGGCGAAAAACCGTCTATCAGGGCGATGGCCCACTACGTGAACCATCACCCTAATCAAGTTTTTTGGGGTCGAGGTG
CCGTAAAGCACTAAATCGGAACCCTAAAGGGAGCCCCCGATTTAGAGCTTGACGGGGAAAGCCGGCGAACGTGGCGAGAAAGGAAGGGAAGAAAGCGAAA
GGAGCGGGCGCTAGGGCGCTGGCAAGTGTAGCGGTCACGCTGCGCGTAACCACCACACCCGCCGCGCTTAATGCGCCGCTACAGGGCGCGTCAGGTGGCA
CTTTTCGGGGAAATGTGCGCGGAACCCCTATTTGTTTATTTTTCTAAATACATTCAAATATGTATCCGCTCATGAGACAATAACCCTGATAAATGCTTCA
ATAATATTGAAAAAGGAAGAGTCCTGAGGCGGAAAGAACCAGCTGTGGAATGTGTGTCAGTTAGGGTGTGGAAAGTCCCCAGGCTCCCCAGCAGGCAGAA
GTATGCAAAGCATGCATCTCAATTAGTCAGCAACCAGGTGTGGAAAGTCCCCAGGCTCCCCAGCAGGCAGAAGTATGCAAAGCATGCATCTCAATTAGTC
AGCAACCATAGTCCCGCCCCTAACTCCGCCCATCCCGCCCCTAACTCCGCCCAGTTCCGCCCATTCTCCGCCCCATGGCTGACTAATTTTTTTTATTTAT
GCAGAGGCCGAGGCCGCCTCGGCCTCTGAGCTATTCCAGAAGTAGTGAGGAGGCTTTTTTGGAGGCCTAGGCTTTTGCAAAGATCGATCAAGAGACAGGA
TGAGGATCGTTTCGCATGATTGAACAAGATGGATTGCACGCAGGTTCTCCGGCCGCTTGGGTGGAGAGGCTATTCGGCTATGACTGGGCACAACAGACAA
TCGGCTGCTCTGATGCCGCCGTGTTCCGGCTGTCAGCGCAGGGGCGCCCGGTTCTTTTTGTCAAGACCGACCTGTCCGGTGCCCTGAATGAACTGCAAGA
CGAGGCAGCGCGGCTATCGTGGCTGGCCACGACGGGCGTTCCTTGCGCAGCTGTGCTCGACGTTGTCACTGAAGCGGGAAGGGACTGGCTGCTATTGGGC
GAAGTGCCGGGGCAGGATCTCCTGTCATCTCACCTTGCTCCTGCCGAGAAAGTATCCATCATGGCTGATGCAATGCGGCGGCTGCATACGCTTGATCCGG
CTACCTGCCCATTCGACCACCAAGCGAAACATCGCATCGAGCGAGCACGTACTCGGATGGAAGCCGGTCTTGTCGATCAGGATGATCTGGACGAAGAGCA
TCAGGGGCTCGCGCCAGCCGAACTGTTCGCCAGGCTCAAGGCGAGCATGCCCGACGGCGAGGATCTCGTCGTGACCCATGGCGATGCCTGCTTGCCGAAT
ATCATGGTGGAAAATGGCCGCTTTTCTGGATTCATCGACTGTGGCCGGCTGGGTGTGGCGGACCGCTATCAGGACATAGCGTTGGCTACCCGTGATATTG
CTGAAGAGCTTGGCGGCGAATGGGCTGACCGCTTCCTCGTGCTTTACGGTATCGCCGCTCCCGATTCGCAGCGCATCGCCTTCTATCGCCTTCTTGACGA
GTTCTTCTGAGCGGGACTCTGGGGTTCGAAATGACCGACCAAGCGACGCCCAACCTGCCATCACGAGATTTCGATTCCACCGCCGCCTTCTATGAAAGGT
TGGGCTTCGGAATCGTTTTCCGGGACGCCGGCTGGATGATCCTCCAGCGCGGGGATCTCATGCTGGAGTTCTTCGCCCACCCTAGGGGGAGGCTAACTGA
AACACGGAAGGAGACAATACCGGAAGGAACCCGCGCTATGACGGCAATAAAAAGACAGAATAAAACGCACGGTGTTGGGTCGTTTGTTCATAAACGCGGG
GTTCGGTCCCAGGGCTGGCACTCTGTCGATACCCCACCGAGACCCCATTGGGGCCAATACGCCCGCGTTTCTTCCTTTTCCCCACCCCACCCCCCAAGTT
CGGGTGAAGGCCCAGGGCTCGCAGCCAACGTCGGGGCGGCAGGCCCTGCCATAGCCTCAGGTTACTCATATATACTTTAGATTGATTTAAAACTTCATTT
TTAATTTAAAAGGATCTAGGTGAAGATCCTTTTTGATAATCTCATGACCAAAATCCCTTAACGTGAGTTTTCGTTCCACTGAGCGTCAGACCCCGTAGAA
AAGATCAAAGGATCTTCTTGAGATCCTTTTTTTCTGCGCGTAATCTGCTGCTTGCAAACAAAAAAACCACCGCTACCAGCGGTGGTTTGTTTGCCGGATC
AAGAGCTACCAACTCTTTTTCCGAAGGTAACTGGCTTCAGCAGAGCGCAGATACCAAATACTGTCCTTCTAGTGTAGCCGTAGTTAGGCCACCACTTCAA
GAACTCTGTAGCACCGCCTACATACCTCGCTCTGCTAATCCTGTTACCAGTGGCTGCTGCCAGTGGCGATAAGTCGTGTCTTACCGGGTTGGACTCAAGA
CGATAGTTACCGGATAAGGCGCAGCGGTCGGGCTGAACGGGGGGTTCGTGCACACAGCCCAGCTTGGAGCGAACGACCTACACCGAACTGAGATACCTAC
AGCGTGAGCTATGAGAAAGCGCCACGCTTCCCGAAGGGAGAAAGGCGGACAGGTATCCGGTAAGCGGCAGGGTCGGAACAGGAGAGCGCACGAGGGAGCT
TCCAGGGGGAAACGCCTGGTATCTTTATAGTCCTGTCGGGTTTCGCCACCTCTGACTTGAGCGTCGATTTTTGTGATGCTCGTCAGGGGGGCGGAGCCTA
TGGAAAAACGCCAGCAACGCGGCCTTTTTACGGTTCCTGGCCTTTTGCTGGCCTTTTGCTCACATGTTCTTTCCTGCGTTATCCCCTGATTCTGTGGATA
ACCGTATTACCGCCATGCAT